1969 SMITHSONIAN STANDARD EARTH (II)

E. M. Gaposchkin and K. Lambeck
Smithsonian Astrophysical Observatory, Cambridge, Massachusetts 02138

1. INTRODUCTION

During 1966 the Smithsonian Astrophysical Observatory (SAO) published numerical parameters for the earth's gravity field and the coordinates of the satellite-tracking stations [Gaposchkin, 1967; Köhnlein, 1967a; Veis, 1967a, b; Whipple, 1967; Lundquist and Veis, 1966]. In 1967, a series of papers by Gaposchkin, Köhnlein, Kozai, and Veis [Lundquist, 1967] produced several refinements to the 1966 solution. This combined effort was the result of some years of improvement in analytical techniques, computer programs, and data acquisition, but since then a major revision of the process and theories has been undertaken. Some of the considerations of the new analysis were reviewed by Gaposchkin [1968], and preliminary results were presented by Gaposchkin [1969], Lambeck [1969a, b], and Gaposchkin and Lambeck [1969]. All these results have now been superseded by the solution presented here, and tests have indicated that these latest results are superior to any previous set of geodetic parameters.

These improvements are the consequences of several advances made since 1966. A significant amount of recent Baker-Nunn data is now available, data that are not only of higher accuracy but that also have a better geographic distribution. The latter is due in part to relocation of four Baker-Nunn cameras (9028, 9029, 9031, and 9091), cooperation with some additional observatories, and careful selection of observing periods that yield an optimum distribution and density of observations. The increase in available

data was particularly important for the geometric solution, where, for the first time, a global triangulation net has been established relating all the Baker-Nunn stations except the one in Australia. A further significant improvement in the new solution is due to the incorporation of highly accurate laser range data on six satellites.

As before, the geodetic parameters are estimated from a combined solution of the results obtained by the geometric and dynamic methods. In addition, the combination solution includes station-position information determined by the Jet Propulsion Laboratory (JPL) for its Deep Space Tracking Network (DSN) and surface-gravity anomalies computed by Kaula [1966a]. The final solution yields harmonic coefficients in the potential expansion complete to degree and order 16, plus 14 pairs of higher degree coefficients and the coordinates for 39 stations. This solution has been compared with recent surface-gravity data and astrogeodetic data. Figure 1 gives the locations of the stations used in this analysis.

The next section of this report deals with data collection and reduction, the reference systems, and the accuracy of the data, all of which are important for the understanding of the results. The following four sections discuss the dynamic solution, the geometric solution, the data obtained from the DSN, and the surface-gravity data, while the next section discusses the combination procedure, the results obtained and their evaluation. Our conclusions based on this solution are given in the final section.

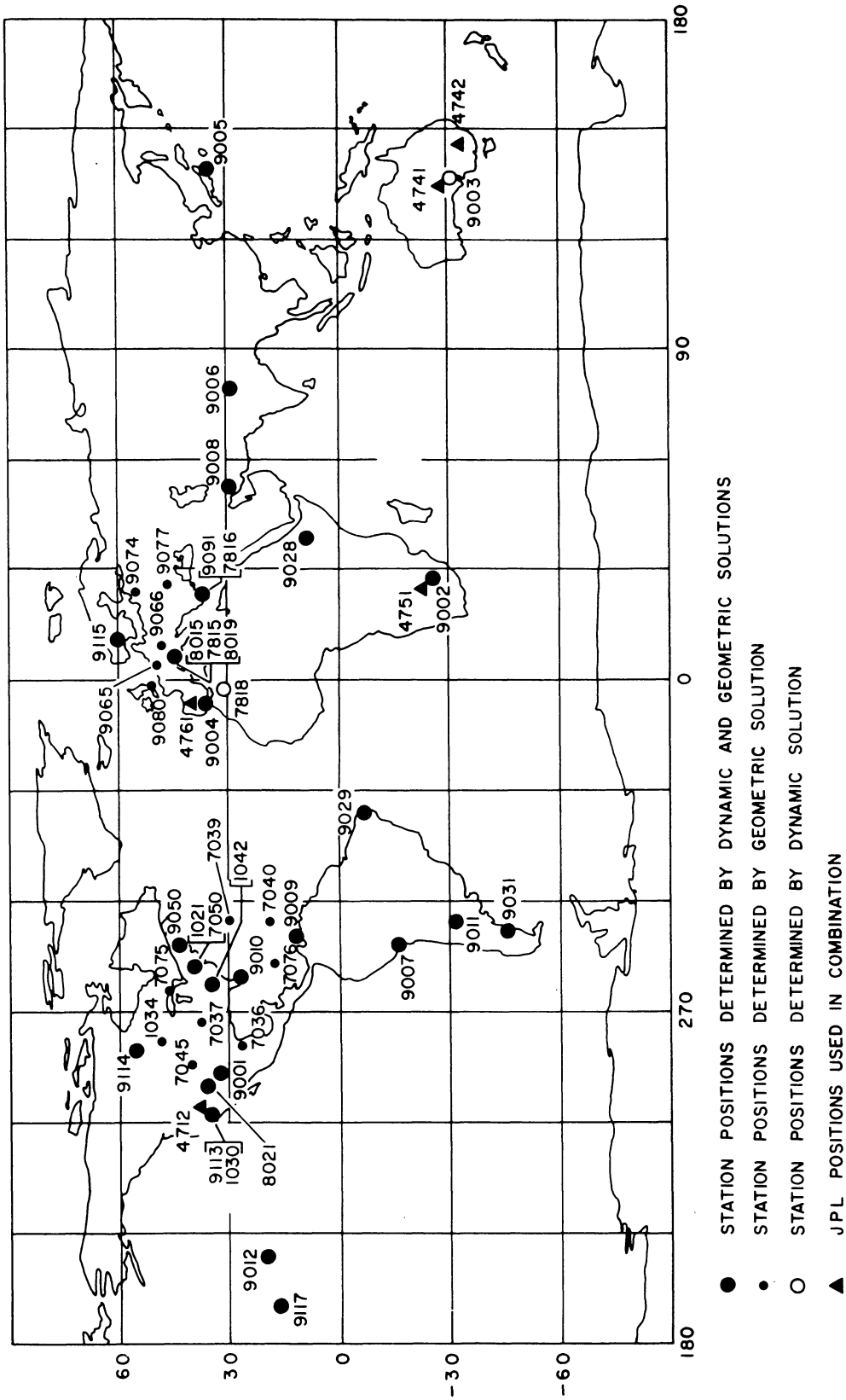

Fig. 1. Location of stations used in the combination solutions. Collocated stations are bracketed together.

2. DATA COLLECTION, REDUCTION, AND REFERENCE SYSTEM

Data Collection

For observations used in the dynamic solution, a new mode of data acquisition has resulted in a better distribution and a higher density of observations along the orbit. With the use of long-range forecasts, intervals of 30 days or longer are chosen during which most of the stations can observe the satellite. More predictions are generated (three per pass), and the satellite is placed on a high-priority observing status. The Baker-Nunn camera takes five to seven frames, and normally the best frame is chosen for reduction. For selected files, all frames are measured, as are observations of the flashing lamps of the Geos 1 and Geos 2 satellites. The multiple-frame reductions are used to obtain synthetic observations [Aardoom, Girnius, and Veis, 1966], and the select files are made up entirely of these data.

Laser tracking systems have been developed in the last 4 years and coordinated observing periods established in 1967, 1968, and 1969. The select files include significant amounts of laser data.

Since 1966, predictions for observations for the geometric solution are made only when the station-satellite configurations meet certain optimum conditions [Lambeck, 1966].

In addition to data from the SAO Baker-Nunn and laser networks, data collected by other agencies have also been used:

1. Laser data from stations 7815, 7816, and 7818 were made available by the Centre National d'Etudes Spatiales (CNES), France.

2. Laser data from station 7050 were made available by the Goddard Space Flight Center (GSFC).

3. Optical data were obtained from the following European stations: 8015 and 8019 (Observatoire de Paris); 9065 (Technical University of Delft); 9066 (Astronomical Institute, Berne); 9074 and 9077 (USSR Astronomical Council); and 9080 (Royal Radar Establishment, Malvern).

4. Optical data from the MOTS cameras 1021, 1030, 1042, 7036, 7037, 7039, 7040, 7075, and 7076 were supplied by GSFC.

Data Reduction

The reduction of the optical data was carried out with all terms in precession and nutation necessary to ensure that the maximum neglected effect is less than 0.5 m. Annual aberration is added and diurnal aberration must be applied to the simultaneous observations. Parallactic refraction was applied by the use of mean nighttime temperature and pressure taken at each station to establish the refraction coefficient [G. Veis, private communication, 1966]. Systematic corrections to star-catalog positions were applied where appropriate. All optical data received from other agencies were corrected in the same way.

The laser observations were reduced by use of the corrections described in Lehr [1969].

Reference System

SAO has its own master clock and through VLF transmission maintains its own coordinated time system called A.S. The principal time reductions were to convert the Goddard laser data from UTC to A.S and the French laser data from A3 to A.S.

The UT1 data used in 1966 were a combination of final and preliminary values of the United States Naval Observatory (USNO). An examination of the differences between the USNO values and those of the Bureau International de l'Heure (BIH) revealed differences approaching 5 m. For the present

solution, BIH UT1 values have been adopted throughout. It appears that these data may be a limiting factor for the ultimately attainable accuracy of station positions.

The polar-motion data were taken from the International Polar Motion Service (IPMS). The difference between these and the BIH data for the period since they were referred to the same origin is as much as 1.5 m. The IPMS data used here were all referred to the mean pole of 1900-1905.

The coordinate system used is the equator of date and the equinox of 1950.0. The choice of this system is discussed further in Section 3. The position of the earth with respect to this system was tabulated in terms of the UT1 and polar-motion data.

Initial Values

As in 1966, the determination of the zonal harmonics was a precursor to this analysis. With use of the 1966 solution, the orbital information was completely revised. Kozai's [1969] zonal harmonics to J(21) were used as starting values. The coefficients are listed for reference in Table 1. Also given are the adopted values for GM, a_e, and the velocity of light c.

Computation of the Synthetic Observations

The methods used earlier at SAO for computing the synthetic direction have remained essentially unchanged [Aardoom et al., 1966]. The satellite is observed at successive instants, usually from 5 to 7, a polynomial is fitted to the reduced positions, and an interpolation is made for some intermediate instant. Usually from 5 to 7 observations are made separated by time intervals ranging from 4 to 16 sec, depending on the velocity of the satellite. A second-order curve fit is found to be adequate for describing the apparent motion during the sequence. For simultaneous observations, the synthetic simultaneous position is computed from overlapping series of observations taken from two or more stations.

TABLE 1. Adopted zonal harmonics to J(21) [Kozai, 1969].

J(2) = 1.08262800E-03	J(3) = -2.5380E-06
J(4) = -1.5930E-06	J(5) = -2.3000E-07
J(6) = 5.0200E-07	J(7) = -3.6200E-07
J(8) = -1.1800E-07	J(9) = -1.0000E-07
J(10) = -3.5400E-07	J(11) = 2.0200E-07
J(12) = -4.2000E-08	J(13) = -1.2300E-07
J(14) = -7.3000E-08	J(15) = -1.7400E-07
J(16) = 1.8700E-07	J(17) = 8.5000E-08
J(18) = -2.3100E-07	J(19) = -2.1600E-07
J(20) = -5.0000E-09	J(21) = 1.4400E-07

$GM = 3.986013 \times 10^{20}$ cm^3/sec^2

$a_e = 6.378155 \times 10^{6}$ m

$c = 2.997925 \times 10^{10}$ cm/sec

Accuracies of the Observational Data

The accuracy of a single Baker-Nunn observation has been nominally set to 4 arcsec, though the more recently collected data are better than this. Accuracy estimates for the synthetic positions are derived from the least-squares curve-fitting procedures. However, these estimates tend to be overoptimistic since they do not reflect possible systematic errors in the entire sequence — for example, timing of the instant of observation, star catalog uncertainties, or anomalous refraction [Lambeck, 1969a]. An analysis of simultaneous observations indicates that these systematic errors average about 0.5 arcsec in the across-track component and $[(0.5)^2 + \dot{\chi}^2 \sigma_t^2]^{1/2}$ for the along-track component, where $\dot{\chi}$ is the apparent angular velocity of the satellite and σ_t is the timing uncertainty of the order 1 to 2 msec. In the geometric solution the accuracy estimates of the synthetic directions have been modified accordingly. The estimates range from

about 1 to 3 arcsec. The laser range data are considered accurate to about 2 m [Lehr, 1969], but the influence of timing errors at the stations has to be considered. For passes with more than 10 observed points, 10 points equally spaced in the pass are selected. To account for redundancy and systematic errors of the laser data, the assumed accuracy of each laser point is taken at 5 m for the SAO and GSFC laser data and at 10 m for the CNES data.

3. DYNAMICAL SOLUTION

The trajectory of a satellite is determined by the forces acting on it and by its initial conditions; stated mathematically in terms of Newton's law,

$$\underset{\sim}{F} = m \underset{\sim}{a} \quad ,$$

which is a family of differential equations. The more familiar form is

$$\ddot{\underset{\sim}{r}} = F(\underset{\sim}{r}, \dot{\underset{\sim}{r}}, t) \tag{1}$$

with suitable initial conditions.

The main problem in celestial mechanics is to develop formulas (a theory in this nomenclature) that predict the trajectory when the forces and the initial conditions are established. This is very difficult and, in general, we must be satisfied with approximate solutions, which for our purpose are quite satisfactory. Alternatively, a direct numerical integration of equation (1) could be carried out.

The forces we consider are the gravitational attraction of the earth, moon, and sun, and the nongravitational effects of radiation pressure and air drag. In this analysis we have chosen satellites that are dominated by the geopotential and for which other effects can, in some way, be assumed known.

The gravity field of the earth, or equivalently the geopotential, is quite irregular. The geopotential V can be represented as an infinite series of spherical harmonics, and the form adopted for this analysis is

$$V = \frac{GM}{r}\left[1 - \sum_{n=2}^{\infty} J_n \left(\frac{a_e}{r}\right)^n p_n(\sin\phi) + \sum_{\ell=2}^{\infty}\sum_{m=1}^{\ell}\left(\frac{a_e}{r}\right)^{\ell} P_{\ell m}(\sin\phi)(C_{\ell m}\cos m\lambda + S_{\ell m}\sin m\lambda)\right], \quad (2)$$

where GM is the product of the gravitational constant and the mass of the earth, ϕ, λ are earth-fixed latitude and longitude, a_e is the equatorial radius of the earth, and

$$p_n(\sin\phi) = \frac{1}{2^n}\sum_{k=0}^{r}(-)^k \frac{(2n-2k)!}{k!\,(n-k)!\,(n-2k)!}\sin^{n-2k}\phi,$$

where r is the greatest integer $\leq n/2$,

$$P_{\ell m}(\sin\phi) = \sqrt{\frac{2(2\ell+1)(\ell-m)!}{(\ell+m)!}}\,\frac{\cos^{\ell}\phi}{2^{\ell}}\sum_{k=0}^{r}(-)^k \frac{(2\ell-2k)!}{k!\,(\ell-k)!\,(\ell-m-2k)!}\sin^{\ell-m-2k}\phi,$$

where r is the greatest integer $\leq (\ell - m)/2$. Expression (2) uses a mixed normalization. The expression $P_{\ell m}(\sin\phi)$ is the fully normalized associated Legendre polynomial, i.e.,

$$\int_{\text{sphere}} P^2_{\ell m}(\sin\phi)\begin{Bmatrix}\sin m\lambda\\ \cos m\lambda\end{Bmatrix}^2 d\sigma = 4\pi, \quad m \neq 0,$$

and $C_{\ell m}$, $S_{\ell m}$ are fully normalized coefficients, as previously published (sometimes designated as $\overline{C}_{\ell m}$, $\overline{S}_{\ell m}$). The $p_n(\sin\phi)$ are the conventional Legendre polynomials and the J_n are conventional harmonics. To include the J_n in the fully normalized form we have

$$P_{\ell 0} = \sqrt{2\ell + 1}\ p_\ell$$

and

$$C_{\ell 0} = -\frac{J_\ell}{\sqrt{2\ell + 1}} \quad ,$$

and the summation in equation (2) would be $m = 0, 1, 2, \ldots, \ell$. The $C_{\ell m}$, $S_{\ell m}$ are called tesseral harmonics, and the J_n are called zonal harmonics. For a systematic development see Heiskanen and Moritz [1967].

In equation (2) we assume $J_1 = C_{21} = S_{21} = 0$ because the origin of the coordinate system chosen is referred to the earth's center of mass, and the z axis ($\phi = \pi/2$) is along the principal axis, i. e., the axis of maximum moment of inertia. In fact, these are only assumptions and one can only approximately realize such a coordinate system.

We use some striking properties of the coefficients to construct the analytical theory by the method of successive approximations. We deal with satellites whose ratio r/a_e lies between 1.1 and 2 and note that J_2 is of the order 10^{-3} and $J_n (n \neq 2)$, $C_{\ell m}$, $S_{\ell m}$ are of the order 10^{-6}. Then, broadly speaking, the motion is dominated by the central force term GM/r and the major additional effect is due to J_2, other gravitational terms being considerably smaller. The successive approximations are indicated by this ordering.

Observations of a satellite depend on the position of the satellite and the observer and on the nature of the observation. The positions are imperfectly known, because of station-coordinate uncertainties, limited knowledge of the satellite's geocentric position vector $\underset{\sim}{r}$, and measurement errors. We limit this analysis to observers fixed to the "solid" earth. This system of sites defines the earth-fixed reference system.

If we denote the geocentric position vector of the observer by $\underset{\sim}{R}$ and the (partially) observed topocentric satellite-position vector by $\underset{\sim}{\rho}$, then these vectors and $\underset{\sim}{r}$ must satisfy the simple relation $\underset{\sim}{\rho} = \underset{\sim}{r} - \underset{\sim}{R}$.

Equation (1) has the simplest form if expressed in an inertial reference frame. The earth has a complicated motion in such a frame because of precession, nutation, polar motion, and rotation. A convenient reference frame is defined by the stars and, in practice, is defined (imperfectly) in terms of a star catalog at some epoch. On the other hand, in an inertial frame the earth's gravity field has a temporal variation that significantly complicates the construction of an analytical theory. It is for this reason that a compromise quasi-inertial reference frame referred to an equinox (epoch of 1950.0) and an equator (epoch of date) is adopted. Veis knew, Kozai proved, and we have used the fact that this coordinate system minimizes the additional effects required to account for the temporal variations of the gravity field and the noninertial property of the coordinate system.

The elaboration of the analytical theory is distinct from the subject to be discussed here. The analytical theory of celestial mechanics has its origins with Lagrange and Hamilton. The process, in one form or another, involves expressing equation (1) in harmonic functions and expansions in terms of a small parameter. These harmonic functions are then suitable for approximate integration. For theoretical and practical reasons the terms are classified by their period. Hence we talk of short-period terms, long-period terms (i.e., terms with period much longer than the orbital period), and terms that do not have a periodic character. This last class includes the secular terms, decay terms due to nongravitational effects, and probably parts of very-long-period terms not modeled in the analytical theory as such and arising as the polynomial expansion of sin x.

The five classes of forces mentioned above are smaller than the principal term (GM/r) for the satellites considered. Departures of the motion from the closed-form elliptical solution are treated as perturbations. The objective of the analytical theory is to determine the perturbations.

The J_n give rise to all classes of terms. The dominant perturbations are the secular effects due to J_{2n}, and in practice these harmonics are determined from observations of the secular perturbations. The J_{2n+1} give rise to long-period terms, with period of the motion of perigee (ω), and are similarly determined from observations of the long-period perturbations. The $C_{\ell m}$ $S_{\ell m}$ give rise to short-period terms only, and the other forces to all three effects.

The development of perturbations, now classical, is given in many papers (e.g., Kaula [1966b]). The choice of dependent variables is arbitrary. The most common are ω (perigee), Ω (argument of the node), I (inclination), e (eccentricity), M (mean anomaly), and a (semimajor axis). These elements ε_i can be combined into any other set. For descriptive purposes we use M and the shift in position $dr = (\overline{dr} \cdot \overline{dr})^{1/2} = \hat{dr} \cdot \overline{dr}$.

The expression of a periodic perturbation (say in M) due to harmonic $C_{\ell m}$ is given in the form

$$\delta M_{\ell m} = C_{\ell m} \sum_{p=0}^{\ell} \sum_{q=-\infty}^{\infty} A(\ell, m, p, q, a, e, I) \mathcal{S}[(\ell - 2p)\omega + (\ell - 2p + q)M + m(\Omega - \theta)] \tag{3}$$

or

$$\delta M_{\ell mpq} = C_{\ell m}\, \delta M^{*}_{\ell mpq}\, \mathcal{S}[(\ell - 2p)\omega + (\ell - 2p + q)M + m(\Omega - \theta)] \quad , \tag{4}$$

where $\mathcal{S}$ is either sin or cos and θ is the sidereal angle.

A few well-known remarks follow:

1. $A(\ell, m, p, q, a, e, I) \propto e^{|q|}$; hence the largest terms generally come with $q = 0$.

2. The q summation, though formally from $-\infty$ to $+\infty$, only needs to go from -10 to +10.

3. $n \cong \dot{M} > \dot{\theta} \approx 1 \gg \dot{\omega}, \dot{\Omega}$; therefore the frequency

$$f = \frac{(\ell - 2p)\dot{\omega} + (\ell - 2p + q)n + m(\dot{\Omega} - \dot{\theta})}{2\pi}$$

of any term is mainly controlled by $\dot{M}$ and $m\dot{\theta}$.

4. Since $A(\ell, m, p, q, a, e, I)$ depends on elements that have virtually no change, A is constant for any particular satellite. The $\dot{S}$ term contains all the temporal variations.

5. Apart from commensurabilities in $n - m\dot{\theta}$ (the resonant case), long-period terms can arise only with $m = 0$, i. e., the zonal harmonics.

Frequency Decomposition

For any given value of order m, all perturbations of degree ℓ even will have the same frequency. Since $0 \leq m \leq \ell$ and $0 \leq p \leq \ell$, arguments with $\ell - 2p = r$ exist. This can be seen by examining the dominant term for each ℓ, i. e., $q = 0$. The frequency becomes

$$f = \frac{(\ell - 2p)(\dot{\omega} + n) + m(\dot{\Omega} - \dot{\theta})}{2\pi} .$$

With $\ell = 12$, $p = 6$, and $m = 12$, we have the same frequency as with $\ell = 14$, $p = 7$, and $m = 12$; $\ell = 16$, $p = 8$, and $m = 12$; etc., similarly for ℓ odd. In addition, we cannot have the same period for both ℓ odd and ℓ even.

For example, the perturbations in M for D1D (6701401) are given in Equation (5) for only the principal terms with $m = 1, 2$; $\ell = 3, 4, 5, 6, 7, 8$. For this satellite, $a = 7614$ km, $e = 0.0843$, and $I = 39.^{\circ}455$.

$$\delta M = C_{31}[-7.1 \sin(\omega + \Omega - \theta) + 0.8 \sin(\omega + 2M + \Omega - \theta) - 63.3 \sin(-\omega + \Omega - \theta) + \ldots]$$

$$+ C_{32}\{-42.5 \cos[\omega + 2(\Omega - \theta)] + 10.5 \cos[\omega + 2M + 2(\Omega - \theta)] - 13.6 \cos[-\omega + 2(\Omega - \theta)] + \ldots\}$$

$$+ C_{41}[7.0 \cos(-M + \Omega - \theta) - 8.2 \cos(M + \Omega - \theta) + 5.1 \cos(-2\omega + \Omega - \theta) + \ldots]$$

$$+ C_{42}\{-10.3 \sin[-M + 2(\Omega - \theta)] + 14.2 \sin[M + 2(\Omega - \theta)] + \ldots\}$$

$$+ C_{51}[-87.4 \sin(\omega + \Omega - \theta) + 6.9 \sin(\omega + 2M + \Omega - \theta) + 87.9 \sin(-\omega + \Omega - \theta) + \ldots]$$

$$+ C_{52}\{8.6 \cos[\omega + 2(\Omega - \theta)] - 1.4 \cos[\omega + 2M + 2(\Omega - \theta)] + 43.9 \cos[-\omega + 2(\Omega - \theta)] + \ldots\}$$

$$+ C_{61}[5.1 \cos(-M + \Omega - \theta) - 6.0 \cos(M + \Omega - \theta) - 16.2 \cos(-2\omega + \Omega - \theta) + \ldots]$$

$$+ C_{62}\{5.4 \sin[-M + 2(\Omega - \theta)] - 7.4 \sin[M + 2(\Omega - \theta)] + \ldots\}$$

$$+ C_{71}[33.1 \sin(\omega + \Omega - \theta) + 0.0 \sin(\omega + 2M + \Omega - \theta) + 1.4 \sin(-\omega + \Omega - \theta) + \ldots]$$

$$+ C_{72}\{40.0 \cos[\omega + 2(\Omega - \theta)] - 5.5 \cos[\omega + 2M + 2(\Omega - \theta)] - 40.3 \cos[-\omega + 2(\Omega - \theta)] + \ldots\}$$

$$+ C_{81}[-6.8 \cos(-M + \Omega - \theta) + 7.9 \cos(M + \Omega - \theta) + 19.1 \cos(-2\omega + \Omega - \theta) + \ldots]$$

$$+ C_{82}\{4.1 \sin[-M + 2(\Omega - \theta)] - 5.7 \sin[M + 2(\Omega - \theta)] + \ldots\} \quad . \tag{5}$$

We can rearrange this expression in terms of the same frequency (with the period P of each term in days given in parentheses):

$$\delta M = (-7.1\, C_{31} - 87.4\, C_{51} + 33.1\, C_{71} + \ldots) \sin(\omega + \Omega - \theta) \quad (-1.001 \text{ days})$$

$$+ (0.8\, C_{31} + 6.9\, C_{51} + 0.0\, C_{71} + \ldots) \sin(\omega + 2M + \Omega - \theta) \quad (0.040)$$

$$+ (-63.3\, C_{31} + 87.9\, C_{51} + 1.4\, C_{71} + \ldots) \sin(-\omega + \Omega - \theta) \quad (-0.971)$$

$$+ (7.0\, C_{41} + 5.1\, C_{61} - 6.8\, C_{81} + \ldots) \cos(-M + \Omega - \theta) \quad (-0.071)$$

$$+ (-8.2\, C_{41} - 6.0\, C_{61} + 7.9\, C_{81} + \ldots) \cos(M + \Omega - \theta) \quad (0.083)$$

$$+(5.1\ C_{41} - 16.2\ C_{61} + 19.1\ C_{81} + \ldots) \cos(-2\omega + \Omega - \theta) \qquad (-0.958 \text{ days})$$

$$+(-42.5\ C_{32} + 8.6\ C_{52} + 40.0\ C_{72} + \ldots) \cos[\omega + 2(\Omega - \theta)] \qquad (-0.497)$$

$$+(10.5\ C_{32} - 1.4\ C_{52} - 5.5\ C_{72} + \ldots) \cos[\omega + 2M + 2(\Omega - \theta)] \qquad (0.041)$$

$$+(-13.6\ C_{32} + 43.9\ C_{52} - 40.3\ C_{72} + \ldots) \cos[-\omega + 2(\Omega - \theta)] \qquad (-0.327)$$

$$+(-10.3\ C_{42} + 5.4\ C_{62} + 4.1\ C_{82} + \ldots) \sin[-M + 2(\Omega - \theta)] \qquad (-0.066)$$

$$+(14.2\ C_{42} - 7.4\ C_{62} - 5.7\ C_{82} + \ldots) \sin[M + 2(\Omega - \theta)] \qquad (0.091)$$

$$+\ldots \quad . \qquad (6)$$

Even if we assume the satellite to be a perfect filter, uncontaminated by other model errors, and the tracking data and analysis process to be perfect, we see that with one satellite we can only determine spectral components that are linear combinations of the gravity field ($C_{\ell m}$) and functions of orbital elements [$A(\ell, m, p, q, a, e, I)$]. From each satellite we obtain one or two linear combinations of harmonics for ℓ odd and for ℓ even. By using additional data we can only refine the numerical value of these linear combinations. The coefficients of the relations will depend on the orbital elements so that other linear combinations can be determined only from additional distinct orbits. Generally, this is achieved by selecting satellites with different inclination, but independent linear relations can also be obtained with changes in eccentricity e or semimajor axis a.

As the degree increases, the perturbations become negligible, and so the linear relation does not involve an infinite number of parameters. Of course, the spectrum analysis gives both amplitude and phase, or as is generally written, a sine and a cosine term.

From equation (6) we see that a linear combination of C_{31}, C_{51}, C_{71}, ... can be determined from the -1.001-day-period term and another of equal size from the -0.971-day term. The third term, and there are many smaller terms, is a factor of 10 smaller and will not contribute significantly as an observation equation. The linear combination of C_{32}, C_{52}, C_{72}, ... has only one significant spectral component for the -0.327-day period.

Therefore, one or two finite linear relations are determined for ℓ odd and one or two for ℓ even. In addition, weaker relations can be established. Each satellite can contribute to the unique determination of 1 or 2 odd and 1 or 2 even degree harmonic coefficients in each order; i.e., if there are 24 sets of unique gravity-field coefficients affecting the orbits for a given order, then between 6 and 12 distinct satellites would be sufficient to determine them.

For a nonhomogeneous set of satellites, i.e., where they are not all equally sensitive to the gravity field, subsets of coefficients are determined. In the case where insufficient satellites are available, the linear relations are generally solved by constraining the higher degree and order coefficients to zero.

The linear relations are not determined with equal accuracy; for example, the resonant harmonics have a very large effect and the spectral component is strongly determined. However, the resonant period is commensurate with the arc length, which will cover only a small number of cycles. This makes separating nearly commensurate periods difficult. For spectral components bunched between P = 0.02 and P = 0.04 day, i.e., between 50 and 60 min, the effects are small and the spectral decomposition is also difficult.

Resonance

Equations (1) for the tesseral harmonics written in the equivalent form of Lagrange planetary equations are integrated, assuming a precessing Keplerian ellipse, as a forced harmonic oscillator. The time enters the

right-hand side of the equation through the rotation of the earth. This forced harmonic oscillator may have a resonance that will change the character of the motion. A resonance was not anticipated and was observed before it was explained analytically. We turn to the analytical theory for some insight into this problem. The expression for $A(\ell, m, \ldots)$ in equation (3), or $M^{*}_{\ell mpq}$ in equation (4), can be further broken down as $A'/[(\ell - 2p)\dot{\omega} + (\ell - 2p + q)n + m(\dot{\Omega} - \dot{\theta})]$. The resonance is associated with the order m and occurs mathematically because $\dot{\omega}$ and $\dot{\Omega}$ are small, $\dot{\theta} \approx 1$ rev/day, and $m \times \dot{\theta} \approx n$, if n is roughly an integral number of revolutions per day. The combination $n - m\dot{\theta}$ can then become arbitrarily small. As the denominator is the time derivative of the argument in equation (2), the larger the amplitude the longer will be the period. Therefore, all harmonics of order m will be resonant with a satellite of mean motion $n \cong m$.

Resonant terms occur in satellite theory and in planetary theory, and there is an extensive literature on the subject (e. g., Kaula [1966b]; Hagihara [1961]), but as yet there is no completely satisfactory treatment. It is true, for example, that a solution such as that employed here using linearized equations can be invalid for some cases, since the series are not uniformly convergent, but fortunately this does not occur here.

The resonant terms are grouped by period in the same way as the periodic terms illustrated by equation (6). Therefore, with n satellites resonant with a given order of the gravity field, we can determine 2n sets of harmonic coefficients.

The occurrence of resonances between the gravity field of the earth and a satellite has been viewed as an opportunity to determine particular harmonics with high precision. In fact, some of the low-degree harmonics have been studied extensively with synchronous satellites, and many harmonics of order 12, 13, and 14 have been determined by SAO and others. Satellites with strong resonances interact with the gravity field to $\ell = 25$ and higher. The large number of harmonics affecting a satellite is related by a linear equation similar to equation (6). For one satellite only a linear combination

of coefficients can be determined. In those cases where insufficient satellites are observed, then, to obtain independent equations, other assumptions are necessary — usually that some of the higher degree terms are set to zero, leading to "lumped" coefficients that are useful for orbit determination but are generally unrelated to the actual gravity field.

The formal theory we employ accounts for both resonances and short-period terms. The occurrence of very large, long-period terms in the theory is possible. For example, the perturbation in mean anomaly for the satellite 5900701 is

$$\delta M = C_{11,11}\left\{-1.387 \times 10^{2} \cos\left[\frac{2\pi}{35.8}(t - t_0)\right]\right.$$

$$\left. - 1.798 \times 10^{5} \cos\left[\frac{2\pi}{1124.8}(t - t_0)\right] + \ldots\right\} , \qquad (7)$$

with similar terms for $S_{11,11}$, $C_{12,11}$, ... The 1124-day term is much longer than any span of data for one orbit. Because we have no knowledge of the coefficient $C_{11,11}$, the empirical orbit would absorb the 1124-day term into the mean elements. It would, therefore, not be reflected in the residuals of the orbit. The observation equation is normally of the form

$$d\bar{x} = \left(\frac{\partial \bar{r}}{\partial m}\frac{\partial \delta M}{\partial C_{\ell m}} + \frac{\partial \bar{r}}{\partial \omega}\frac{\partial \delta \omega}{\partial C_{\ell m}} + \ldots\right) \Delta C_{\ell m} \quad ,$$

which would contain the 1124-day period. Obviously, the process would be faulty. The remedy is to ignore in the analytical theory all perturbations that would be absorbed in the mean elements. With the theory developed in harmonic functions, the deleting of specific perturbations is quite trivial. The analogous operation with a numerical integration technique would be much more difficult.

Evaluation of the Geopotential

The process of gravity-field determination begins with evaluating the secular and long-period perturbations to determine the J_n. The perturbations accumulate for weeks and months, and the effects are very large. The mean orbital elements, determined from overlapping 4-day arcs, are the basic data used in the analysis. Data and reference orbits of moderate accuracy are adequate for the J_n determination. The unbiased recovery of the J_n requires painstaking evaluation of the long-period and secular perturbations from other sources. These are principally due to solar radiation pressure, atmospheric drag, and lunar and solar attraction. This phase of the analysis is accomplished first and forms the basis for the work discussed here. An excellent review of the J_n determination is given by Kozai [1966], and the most recent results are given in Table 1 of Kozai [1969].

The tesseral harmonics are determined from the short-period (1 revolution to 1 day) changes in the orbit. The detailed structure of the orbit must be observed, and each observation provides an observation equation. Data of the highest possible precision are needed.

The unbiased recovery of the $C_{\ell m}$, $S_{\ell m}$ requires the evaluation of the periodic terms from other sources that have periods similar to those arising from the gravity-field coefficients. The most important terms are the short-period terms due to J_n and the lunar attraction. Because they are smaller than 1 m for the satellites used in this analysis, the periodic effects of air drag and radiation pressure can be ignored. The nonperiodic terms are empirically determined and hence are accounted for. The short-period terms due to J_2 must be carried to second order. Further details on the analytical theory will appear separately.

We have the basic relation

$$[A]\,\bar{\rho}(t) = [A]\,[\bar{r}(C_{\ell m},\ S_{\ell m},\ \varepsilon_i,\ t) - \bar{R}(t)] \quad , \tag{8}$$

where the matrix operation [A] transforms $\bar{\rho}$ to our observed quantity, either a direction or a range. With an orbital theory, we can develop (8) in a series about initial values of ε_i^0, $C_{\ell m}^0$, $S_{\ell m}^0$, and R_i^0:

$$[A]\ d\bar{\rho}(t) = [A]\left(\frac{\partial \bar{r}}{\partial C_{\ell m}}\ \Delta C_{\ell m} + \frac{\partial r}{\partial S_{\ell m}}\ \Delta S_{\ell m} + \frac{\partial r}{\partial \varepsilon_i}\ \Delta\varepsilon_i - \frac{\partial \bar{R}}{\partial R_i}\ \Delta R_i\right) ,$$

where

$$\frac{\partial \bar{r}}{\partial C_{\ell m}} = \frac{\partial \bar{r}}{\partial \varepsilon_i}\ \frac{\partial \varepsilon_i}{\partial C_{\ell m}} \qquad \text{by the chain rule.}$$

From equations (2), (3), (6), or (7) we observe that $\partial\varepsilon_i/\partial C_{\ell m} = \partial\delta\varepsilon_i/\partial C_{\ell m}$ is linear in $C_{\ell m}$, and the formula is obtained by omitting the gravity-field coefficient. This linear property is very powerful and would not have occurred if the alternative representation of an amplitude and phase angle had been used for the form of equation (2).

For each orbital arc a set of six mean elements, ε_i, is determined. The linear rates are determined empirically, as are accelerations in perigee, node, and mean anomaly. In addition, higher polynomials in the mean anomaly are employed where appropriate to account for the nonperiodic, yet nonsecular, effects of air drag, radiation pressure, etc., as discussed above. There are 13 or more orbital elements determined for each arc. The arcs range in length from 14 to 30 days. Therefore, with the more than 100 orbital arcs used in this solution there are over 1500 additional parameters to be determined. This can be accomplished without dealing with 2000×2000 matrices by using a device described by Kaula [1966b, p. 104] for reducing the normal equations. For systems of 2000 unknowns, the time required to compute reduced normal equations is much greater than the adopted method, which is a block Gauss-Seidel iteration. Reduced normal equations are used with more limited problems, e. g., solution for resonant harmonics, because it rigorously accounts for the interaction of the elements and unknowns.

The determinations of the orbital elements and the geodetic parameters (gravity field and station coordinates) are separated and iterations are performed alternately, improving one set and then the other. As the iterations proceed, the choice of unknowns is modified: satellites are either deleted or augmented as gravity-field coefficients and station coordinates appear ill determined or significant.

The observation equations are archived arc by arc and combined as the last step. As the normal equations are formed, the solubility of the system is determined. The overdetermined system is solved by the method of least squares. The weighting is given a priori. As the iterations proceed, the weight of certain data sets is modified.

Equation (4) leads us to the method of selecting the gravity-field coefficients that affect the orbit and, therefore, can be determined from observing the orbit. Since $-1 \leq S \leq 1$, $C_{\ell m}$, a, e, and I determine the size of $\delta\varepsilon_{i\ell mpq}$. By using an estimate of $C_{\ell m}$ and the value of the mean elements, we can compute the quantity $\delta\varepsilon^{*}_{i\ell mpq}$. An estimate of $C_{\ell m} = \alpha\ell^{-\beta}$ is used to test for significance and only terms $>\alpha\ell^{-\beta}$ are retained. The $\delta\varepsilon^{*}_{i}$ are all calculated and combined into a shift of position $\sqrt{d\bar{\rho} \cdot d\bar{\rho}}$ and are given in Table 2 for satellite 6701401 with $\ell = 11, 12, \ldots, 20$. The units are adjusted so that with $C_{\ell m}$ expressed in units of 10^{-6} (e.g., $C_{22} = 2.4$), the perturbation in position is in meters. Conservative values for α and β are used, and more terms are carried than perhaps necessary. For example, for $\ell = 11$, $m = 5$, and $C_{\ell m} = 10^{-5}/\ell^{2} = 0.083$, the perturbation is $0.083 \times 38 \approx 3$ m. From such tabulations for each satellite the coefficients that affect the motion of the satellite and determine how many satellites contribute to the determination of a coefficient can be chosen. In addition, the accuracy of the data available controls the size of the effect that can be detected. The choice of coefficients is made by balancing the amount and precision of the data available for a particular satellite with the sensitivity of that satellite to particular coefficients. Further, as the combination with surface gravity proceeded, it became apparent that such information was stronger than the satellite information for some coefficients, and some higher coefficients were dropped from the satellite solution on that basis.

TABLE 2. Sensitivity coefficients for satellite 6701401.

e = 0.0843130 A = 7614 km
I = 39.°45459 Perigee = 594 km
n = 13.064356 Apogee = 1878 km

m \ ℓ	11	12	13	14	15	16	17	18	19	20
1	154	229	121	75	139	160	66	69	118	67
2	113	43	61	94	58	35	59	46	0	33
3	52	78	65	25	54	43	12	18	39	26
4	66	34	19	39	38	14	10	27	0	0
5	38	28	51	29	0	23	10	0	0	18
6	65	48	42	14	27	19	0	17	0	0
7	68	62	61	45	10	0	18	16	0	0
8	46	62	45	37	18	12	0	0	18	0
9	21	30	46	64	55	53	23	0	0	0
10	0	0	29	44	43	58	37	32	0	0
11	0	0	8	16	27	48	47	57	48	44
12		0	0	21	44	64	89	101	75	99
13			425	1203	2987	4758	8014	9531	12277	11613
14				0	0	20	47	77	111	145
15					0	0	0	0	16	20
16						0	0	0	0	0
17							0	0	0	0
18								0	0	0
19									0	0
20										0

Table 2 illustrates two points referred to earlier. The amplitudes for m = 13 are quite large because of the resonance. The large size of the effects continues well into the 20th-degree terms. The m = 12 and m = 14 harmonics also have some effects because they are adjacent to a resonant harmonic.

The station coordinates to be determined are easier to choose. They are limited to those stations that contribute a significant amount of data to all the satellites. Many other stations contributed simultaneous observations that were included in the combined solution. In general, data must be available in considerable amounts for a variety of satellites to give reliable results.

Table 3 details the selection of satellites used in the final solution. They are ordered by inclination. Figure 2 graphically represents the distribution in inclination and perigee height. Many of the satellites are new objects not included in the 1966 solution, while some of the original objects contained new files of data.

The choice of unknowns on the final iteration comprised 290 parameters. The sites treated as a net using survey information were (8015—7815), (9001—7901), (9003—9023), and (9091—7816). The sites selected were the fundamental Baker-Nunn cameras and the laser sites.

Apart from the resonant harmonics, the terms higher than ℓ = 12, m = 12 are weakly determined by the satellite data — when the satellite is low, it is infrequently observed — but it had been demonstrated in earlier iterations that the surface gravity could determine these higher harmonics. The satellite solution was limited to those harmonics that have an effect of greater than 3 to 4 m on the orbit. The resulting terms were complete through ℓ = 12, m = 12, omitting C/S(11, 7); C/S(12, 6); and C/S(12, 9). Higher order terms selected were C/S(ℓ, 1) $13 \leq \ell \leq 16$; C/S(ℓ, 2) $13 \leq \ell \leq 15$; C/S(14, 3); C/S(ℓ, 12) $13 \leq \ell \leq 19$; C/S(ℓ, 13) $13 \leq \ell \leq 21$; C/S(ℓ, 14) $14 \leq \ell \leq 22$.

TABLE 3. Summary of dynamical data.

Satellite	Name or Other Designation	Inclination (deg.)	Eccentricity	Semimajor Axis (km)	Perigee Height (km)	Number of Arcs	Days/Arc	New Satellite	Select Files	Laser Data
6001301	Courier 1B 60 ν1	28	0.016	7465	965	6	30	X	X	
5900101	Vanguard 2 59 α1	33	0.165	8300	557	7	30		X	
6100401	61 δ1	39	0.119	7960	700	3	14			
6701401	D1D	39	0.053	7337	569	6	14	X	X	X
6701101	D1C	40	0.052	7336	579	4	14	X	X	X
6503201	Explorer 27 BE-C	41	0.026	7311	941	4	30	X	X	X
6000902	60 ι2	47	0.011	7971	1512	7	30			
6206001	Anna 1B 62 βμ1	50	0.007	7508	1077	12	30		X	
6302601	Geophysical Research	50	0.062	7237	424	6	14			
6508901	Explorer 29 Geos 1	59	0.073	8074	1121	21	30	X	X	X
6101501	Transit 4A 61 o1	67	0.008	7318	885	8	30			
6101502	Injun 1 61 o2	67	0.008	7316	896	4	30			
6506301	Secor 5	69	0.079	8159	1137	2	30	X	X	
6400101		70	0.002	7301	921	3	30	X		
6406401	Explorer 22 BE-B	80	0.012	7362	912	2	30	X		X
6508101	OGO 2	87	0.075	7344	420	2	14	X		
6600501	Oscar 07	89	0.023	7417	868	1	30	X	X	
6304902	5BN-2	90	0.005	7473	1070	5	30	X		
6102801	Midas 4 61 αδ1	96	0.013	10005	3503	3	50			
6800201	Explorer 36 Geos 2	106	0.031	7709	1101	6	14	X		X
6507801	OV1 2	144	0.182	8306	416	2/114	14	X		

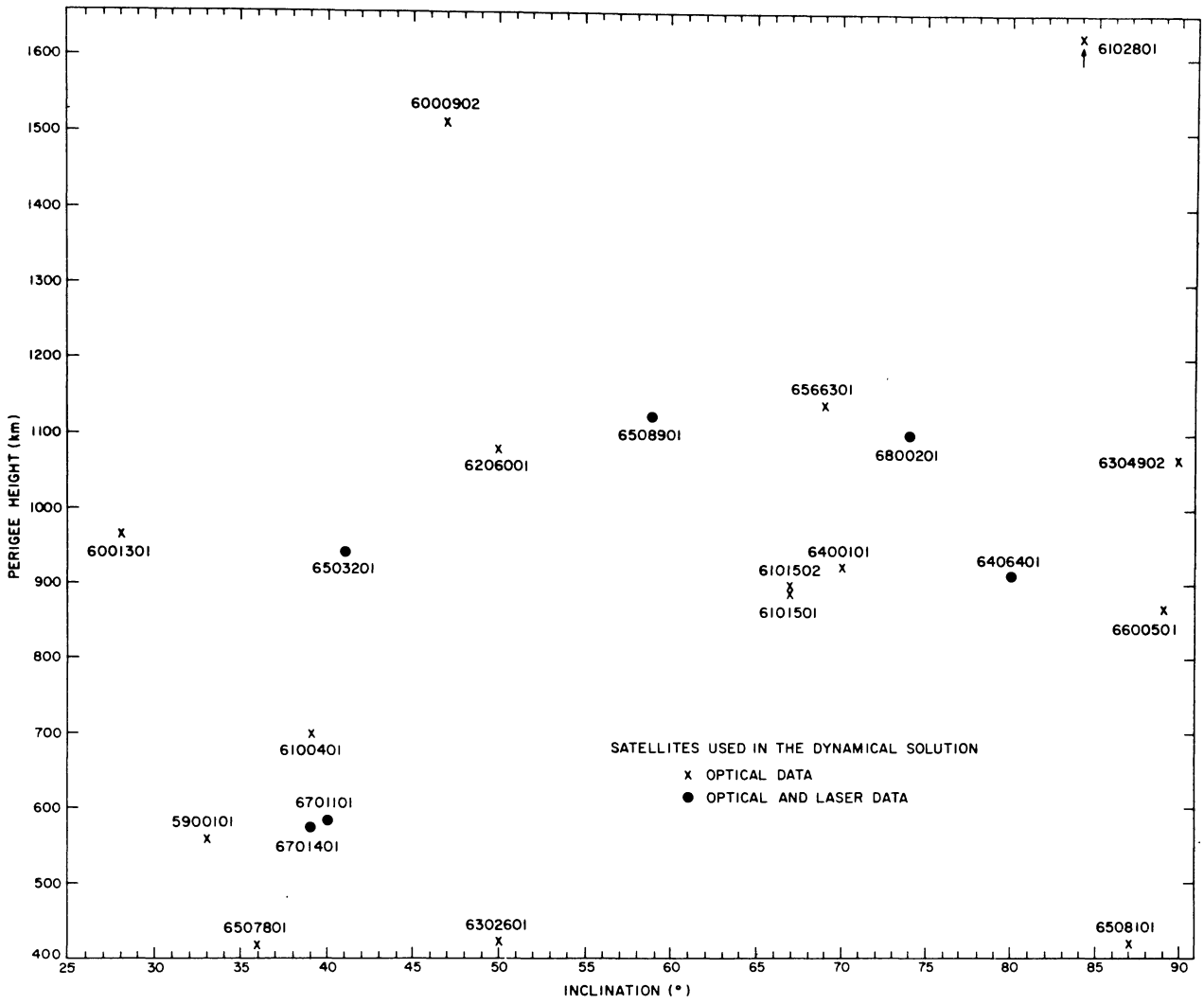

Fig. 2. Distribution of satellites used in the 1969 Smithsonian Standard Earth (II).

The m = 9, 12, 13, 14 terms are resonant with some satellites. Table 4 lists the resonant satellites with their resonant periods. Several satellites are resonant with more than one order. For example, 6701101 has a 1.6-day period with the 13th order and a 2.6-day period with the 14th order, the latter being the principal effect. Other resonances have several periods, as illustrated by equation (7) for 5900701, which was not used in the final solution, and as illustrated in Table 4 for 6701401. The multiple periods are due to the large eccentricity, which causes the frequency splitting.

The results of the dynamical solution must be discussed in the context of the combination solutions. The statistical summary of the data used is given in Tables 3 and 5. The selection of data and unknowns evolved through the analysis. The number of satellites used ranged from 21 to 25, and the number of arcs in the largest solution was 244. Arcs were added and rejected on the basis of contribution to the normal equations, number of observations for a particular station, improvement of distribution for a resonant harmonic, and quality of the orbital fit.

TABLE 4. Resonant periods.

Resonant with Order (m)	Satellite	Inclination (deg.)	Periods (days)
9	6102801	95	2.90
12	6100401	39	15.0
12	6000902	47	15.5
12	6508901	59	7.2
12	6506301	69	3.3
12	6507801	144	2.3
13	6701401	39	9.4, 10.9, 13.1, ...
13	6503201	41	5.6
13	6701101	40	1.6
13	6206001	50	5.3
13	6800201	105	6.3
13	6600501	89	1.8
13	6304901	90	2.5
14	6701101	40	2.6
14	6302601	50	12.2
14	6101501	67	3.84
14	6101502	67	3.76
14	6400101	70	4.9
14	6406401	80	2.9
14	6408101	87	3.8
14	6600501	89	2.2

TABLE 5. Number of observations per station used in the dynamical solution. Final adopted solution.

21 Satellites

114 Arcs

60,456 Observed Quantities

Station Number	Observations	Station Number	Observations
7050	198	9009	1218
7818	964	9010	1936
8015	361	9011	1473
7815	245	9012	2427
9001	3306	9021	143
7901	761	9028	518
9002	2040	9029	277
9003	584	9031	408
9023	2035	9091	459
9004	2950	7816	1017
9005	1010	9113	407
9006	2334	9114	346
9007	1348	9115	215
9008	1302	9117	742

4. GEOMETRIC SOLUTION

The geometric method for determining station positions from observations of satellites does not require any knowledge of the orbit, since the object is observed simultaneously from two or more stations and the relative positions of these stations are computed by a three-dimensional triangulation process. The geometric solution does not give any information on the position of the earth's center of mass, nor does it give a scale determination if only direction observations are used. The solution is further characterized by highly accurate directions between stations, but also by an unfavorable error propagation in station coordinates. When combined with the dynamic solution, the geometric solution contributes significantly to the solution for station coordinates and provides a valuable means of assessing the reliability of these results.

A total of 38 stations was involved in this solution, and 20 of these were also used in the dynamic solution. Observations from 16 SAO and 4 USAF Baker-Nunn cameras, from 13 NASA MOTS cameras, and from 7 European stations were utilized. Approximately 50,000 individual direction observations were used in the analysis, a number comparable to that used in the dynamic solution. Table 6 gives the distribution of the data between the stations. Most of the observations have been made to high-altitude satellites not used in the dynamic solution. These satellites include 6102801 (Midas 4), 6303004, 6605601 (Pageos), and 6805501. For stations closer than about 2500 km, observations in both the passive and the flashing modes of 6508901 (Geos 1) and 6800201 (Geos 2) form the majority of the data.

For stations close together (less than 200 km apart), ground-survey information, when available, was used to impose constraints on their relative positions. This has been done for the following groups of stations: (9051–9091–7816), (1022–7072–9010), (1030–9113), (1021–7043), and (7815–8015–8019).

TABLE 6. Summary of the number of simultaneous events from the Baker-Nunn, K-50, European, and MOTS stations.

Events Observed Simultaneously from Two Baker-Nunn Stations

Stations	No. of Events	Stations	No. of Events	Stations	No. of Events
9001–9007	25	9005–9006	62	9010–9012	2
9001–9009	101	9005–9008	2	9010–9029	6
9001–9010	161	9005–9012	28	9010–9114	38
9001–9012	200	9005–9117	20	9011–9029	19
9001–9113	20	9006–9008	167	9011–9031	12
9001–9114	59	9006–9028	29	9012–9021	32
9001–9117	15	9006-9091	6	9012–9113	14
9002–9008	7	9006–9115	9	9012–9114	24
9002–9028	31	9007–9009	176	9012–9117	241
9002–9091	2	9007–9010	65	9021–9113	61
9004–9006	5	9007–9011	391	9021–9114	7
9004–9008	119	9007–9029	79	9021–9117	6
9004–9009	36	9007–9031	32	9028–9091	41
9004–9010	36	9008–9028	21	9029–9031	21
9004–9028	35	9008–9051	16	9113–9114	49
9004–9029	48	9008–9115	27	9113–9117	18
9004–9051	47	9009–9010	158	9114–9115	5
9004–9091	45	9009–9011	148	9114–9117	2
9004–9114	1	9009–9029	16		
9004–9115	73	9009–9114	9		

Events Observed Simultaneously from Three or More Baker-Nunn Stations

Stations	No. of Events	Stations	No. of Events
9001–9007–9009	2	9004–9008–9115	10
9001–9007–9010	6	9004–9009–9010	7
9001–9007–9009–9010	2	9005–9006–9008	1
9001–9009–9010	82	9005–9012–9117	3
9001–9009–9114	4	9006–9008–9028	1
9001–9010–9012	1	9006–9008–9115	6
9001–9010–9114	9	9006–9028–9091	4
9001–9012–9114	2	9007–9009–9010	20
9001–9012–9117	2	9007–9009–9011	77
9004–9006–9008	5	9007–9011–9029	4
9004–9006–9008–9115	2	9007–9029–9031	1
9004–9006–9115	2	9009–9010–9114	3
9004–9008–9028	6	9012–9021–9117	2

TABLE 6 (Cont.)

Summary of Simultaneously Observed Flashes from Geos 1 and 2 for European Stations

Stations	No. of Events	Stations	No. of Events	Stations	No. of Events
8015–9004	135	8019–9074	86	9065–9080	25
8015–9051	22	8019–9077	10	9065–9091	5
8015–9065	23	8019–9080	10	9066–9074	37
8015–9066	186	8019–9091	79	9066–9077	7
8015–9074	33	9004–9066	203	9066–9080	30
8015–9077	7	9004–9074	41	9066–9091	20
8015–9080	89	9004–9077	19	9074–9077	26
8015–9091	30	9004–9080	139	9074–9080	14
8019–9004	258	9065–9066	12	9074–9091	47
8019–9065	8	9065–9074	32	9077–9091	31
8019–9066	78	9065–9077	4		

Stations	No. of Events	Stations	No. of Events
8015–8019–9004	20	8019–9004–9066	12
8015–8019–9004–9074	2	8019–9004–9066–9091	7
8015–8019–9004–9091	11	8019–9004–9074	11
8015–8019–9065	6	8019–9004–9074–9091	20
8015–8019–9065–9091	4	8019–9004–9091	50
8015–8019–9074	13	8019–9065–9091	1
8015–8019–9077	6	8019–9066–9074	5
8015–8019–9080	1	8019–9077–9091	7
8015–8019–9091	15	8019–9080–9065	6
8015–9004–9051	11	9004–9066–9080	11
8015–9004–9066	27	9004–9066–9091	7
8015–9004–9074	1	9004–9074–9080	5
8015–9004–9080	16	9065–9066–9074	4
8015–9004–9091	5	9065–9066–9074–9077	4
8015–9066–9051	10	9066–9074–9077	7
8015–9004–9066–9080	7	9074–9077–9091	10

TABLE 6 (Cont.)

Summary of Number of Observations per Station for the MOTS Cameras

Station	Number of Flash Sequences Observed	Station	Number of Flash Sequences Observed
1021	85	7045	157
1022	227	7072	86
1030	167	7075	51
1034	166	7076	80
1042	125	9001*	108
7036	149	9009*	19
7037	189	9010*	122
7039	45	9050*	30
7040	67	9113*	70
7043	82	9114*	8

*SAO Geos 1 flash observations, which are simultaneous with MOTS observations.

Method of Adjustment

Because of the Baker-Nunn station locations and satellite-visibility patterns, a majority of the observations are made from only two stations at a time. In the first phase of the adjustment, these observations are used to solve for the directions of the station-station vector. If the n topocentric satellite positions as observed from the two stations are denoted by $\underset{\sim}{\rho}^i_1$ and $\underset{\sim}{\rho}^i_2$ and the unknown station-station vector by $\underset{\sim}{\rho}^i_3$, the condition that these three vectors must satisfy can be expressed simply as

$$(\underset{\sim}{\rho}^i_1 \times \underset{\sim}{\rho}^i_2) \cdot \underset{\sim}{\rho}^i_3 = 0 \qquad (i = 1, 2 \ldots n) \quad .$$

For nearby stations or for very high satellites, simultaneous observations from more than two stations become frequent. This occurs, for example, with observations from the 10 European stations and the 16 North American stations. These observations together with the results obtained

from the first phase are included in the second phase of the adjustment together with any laser range observations. The mathematical model in this case can be written as

$$X_i^j - X_a^j = |\rho_{mia}|\rho_{mia} \qquad \begin{pmatrix} j = 1, 2, 3 \\ i = 1, 2 \ldots n \\ a = 1, 2 \ldots b \end{pmatrix} ,$$

where the X_i^j are the coordinates of the n satellite positions and X_a^j the coordinates of the b stations. The family of equations obtained are solved for the X_a^j after first eliminating the satellite coordinates and any unobserved components of the topocentric position vector.

The Baker-Nunn network is used here as the basic global framework in the adjustment, but because of the station distribution this net is best considered in two parts: the American-Pacific stations (group 1) and the Afro-Eurasian stations (group 2). These two groups link up at San Fernando (9004), at Tokyo (9005), and to a lesser extent at Oslo (9115), so that all the SAO stations with the exception of Woomera (9023) can be connected into one net.

Phase 2 consists of the independent adjustments for the stations in these two groups, as well as for a third group comprising the MOTS data from North America and a fourth group comprising data from the European stations. The reasons for this subdivision are first to isolate and detect possible systematic errors arising from different reduction techniques or instrumentation used in the different data sources, and second to separate the propagation of variances caused by the poor geometry provided by the station positions from the propagation of the variances of the observed quantities.

In the third phase of the adjustment the four groups of stations are linked via common stations. In linking the groups it is only necessary to determine the relative translations and scale. No differential rotations need be considered, since all the data used in this analysis refer to the same astronomical reference system, polar-motion data, and UT1.

The adjustments of the three stages were made by a least-squares procedure, carrying along the full covariance matrices of the functions of the observed quantities from phase to phase. Such a procedure is equivalent to adjusting all the data in a single phase [Tienstra, 1956; Baarda, 1967], but has the advantage of isolating possible systematic errors in the data. If statistical testing of the results of phases 1 and 2 indicated the presence of such errors, the adjustments were further split up in an attempt to locate the faulty data. The statistical testing procedures used followed the ideas of Baarda [1968].

Throughout the adjustment it has been assumed that observations taken at different time instants or from different stations are uncorrelated. Systematic timing errors may prevail over a long period, so that the first assumption is difficult to justify. The second assumption, however, appears generally acceptable, since error in time kept at distant stations is almost always uncorrelated. An analysis of the results of the adjustment of the various phases will indicate whether or not these assumptions are valid.

Results

For the single station-station vector adjustments the average variance factor is 1.5 and varies from 0.7 to 3.1 (Table 7). If no systematic errors are present, the expected value of this quantity should be unity. For example, station-station vectors associated with station 9028 consistently show a large variance factor indicating possible systematic errors in data from this station. The accuracies of the station-station vectors vary between 0.2 and 2 arcsec depending on the number of observations and the station-satellite geometry. Figure 3 plots the accuracies for vectors between SAO Baker-Nunn cameras for which the number of simultaneous events is greater than 30. Also shown are the expected accuracies given by the expression [Lambeck, 1969c, d]

$$\begin{pmatrix} \sigma_V^2 \\ \sigma_A^2 \end{pmatrix} = \frac{\sigma_S^2}{n} \begin{pmatrix} \frac{1}{0.09(L/h) - 0.03} \\ \frac{1}{0.34(L/h) - 0.15} \end{pmatrix} ,$$

where σ_S is the accuracy of a synthetic observation (1.5 arcsec) and L/h is the average ratio of length of station-station vector to satellite height ($\approx$ 1.2); σ_V is the accuracy in the vertical component and σ_A is the accuracy in the azimuth component of the station-station vector, and generally the correlation between these components is small.

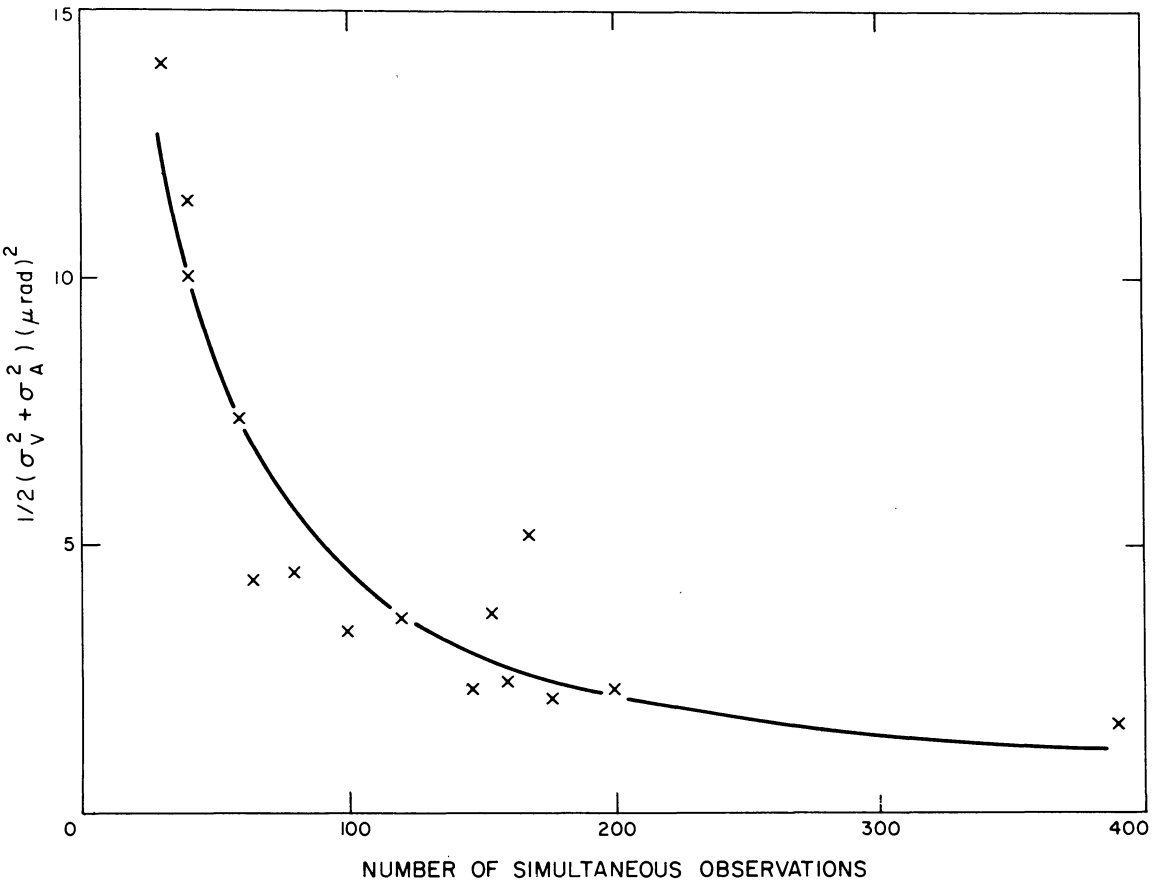

Fig. 3. Mean accuracy of station-station vector as a function of the number of pairs of simultaneous observations used. The crosses mark results obtained from the analysis, and the solid line indicates the expected results for the ratio (station-station distance)/satellite height = 1.2 and the accuracy of a synthetic observation = 7 μrad ($\equiv$ 1.5 arcsec).

TABLE 7. Accuracy estimates for the station-station vectors for which the number of simultaneous pairs of observations n exceeds 27; σ_0^2 is the variance of unit weight of phase 1, σ_1^2 and σ_2^2 are the accuracy estimates of the vectors derived from phase 1 and phase 3, δ^2 is the square of the angular difference between the two estimates, and k^2 is the scaling factor; σ_1, σ_2, and δ are given in μrad.

Line	n	σ_0^2	σ_1^2	σ_2^2	δ^2	k^2
9001–9009	101	1.2	3.4	0.9	12.2	5.5
9001–9010	161	0.9	2.6	1.1	20.4	10.7
9001–9012	200	1.6	2.2	2.6	16.0	6.7
9002–9028	30	3.1	13.8	15.2	7.3	0.5
9004–9008	119	1.2	3.5	1.8	30.4	11.2
9004–9009	36	0.8	9.8	5.4	6.3	0.9
9004–9010	36	0.9	11.4	5.7	7.3	0.9
9004–9028	35	1.9	19.1	3.7	14.4	1.2
9004–9029	48	1.5	22.7	11.0	1.0	0.1
9005–9006	62	0.7	7.1	6.2	1.0	0.2
9005–9012	28	1.3	43.4	23.3	4.0	0.1
9006–9008	167	1.2	5.3	5.3	3.2	0.6
9007–9009	176	1.6	2.2	1.5	9.0	4.7
9007–9010	65	1.6	4.2	1.1	1.0	0.4
9007–9011	391	1.5	2.1	2.7	1.0	0.4
9007–9029	79	1.2	4.5	6.3	9.0	1.7
9007–9031	32	0.9	4.0	6.8	2.2	0.4
9009–9010	158	1.3	3.8	2.5	7.2	2.2
9009–9011	148	2.3	2.4	0.9	3.2	1.9
9012–9117	241	1.6	10.4	16.9	36.0	2.6
9028–9091	41	2.7	18.6	9.3	121.0	8.8
9029–9031	29	1.8	22.0	6.8	17.7	1.2
						$k^2_{AV} = 2.8$

The variances of unit weight for the adjustment in the second phase of the four groups of stations are the following:

group 1: $\sigma_1^2 = 1.39$ (Baker-Nunn, Americas, Pacific, Atlantic)

group 2: $\sigma_2^2 = 1.59$ (Baker-Nunn, Afro-Eurasian)

group 3: $\sigma_3^2 = 0.93$ (European Optical)

group 4: $\sigma_4^2 = 1.99$ (North American MOTS).

Application of the variance ratio tests to the results of phase 2 lead to the general conclusion that, with the exception of the data in group 3, the null hypothesis (i.e., there are no model errors) is to be rejected. However, a reevaluation of the original data gave no indication where the problems may occur, and the results have, of necessity, been accepted.

Finally, the adjustment linking up the four groups of data gives a variance of unit weight equal to 1.4 with 16 degrees of freedom and $F_{0.95,16,\infty} = 1.71$. This suggests that the observations and methods of reduction used in the four groups are compatible.

To investigate further the unsatisfactory conclusions that have to be drawn from the phase 2 adjustments, the directions between stations were computed from the phase 3 results and compared with the phase 1 station-station vectors (see Figure 4). Both these vectors represent estimates of the same quantity, and they can be expected to lie within the accuracy estimates given for them. Comparisons for all the station-station vectors show that this is the case about 60% of the time.

Denoting the mean accuracy of a station-station vector derived from phase 1 by σ_1 and that derived from phase 3 by σ_2, and denoting the angular distance between the two estimates of the vector by δ, we would expect that on the average

$$\delta^2 \leq (1/2)(\sigma_1^2 + \sigma_2^2) \quad .$$

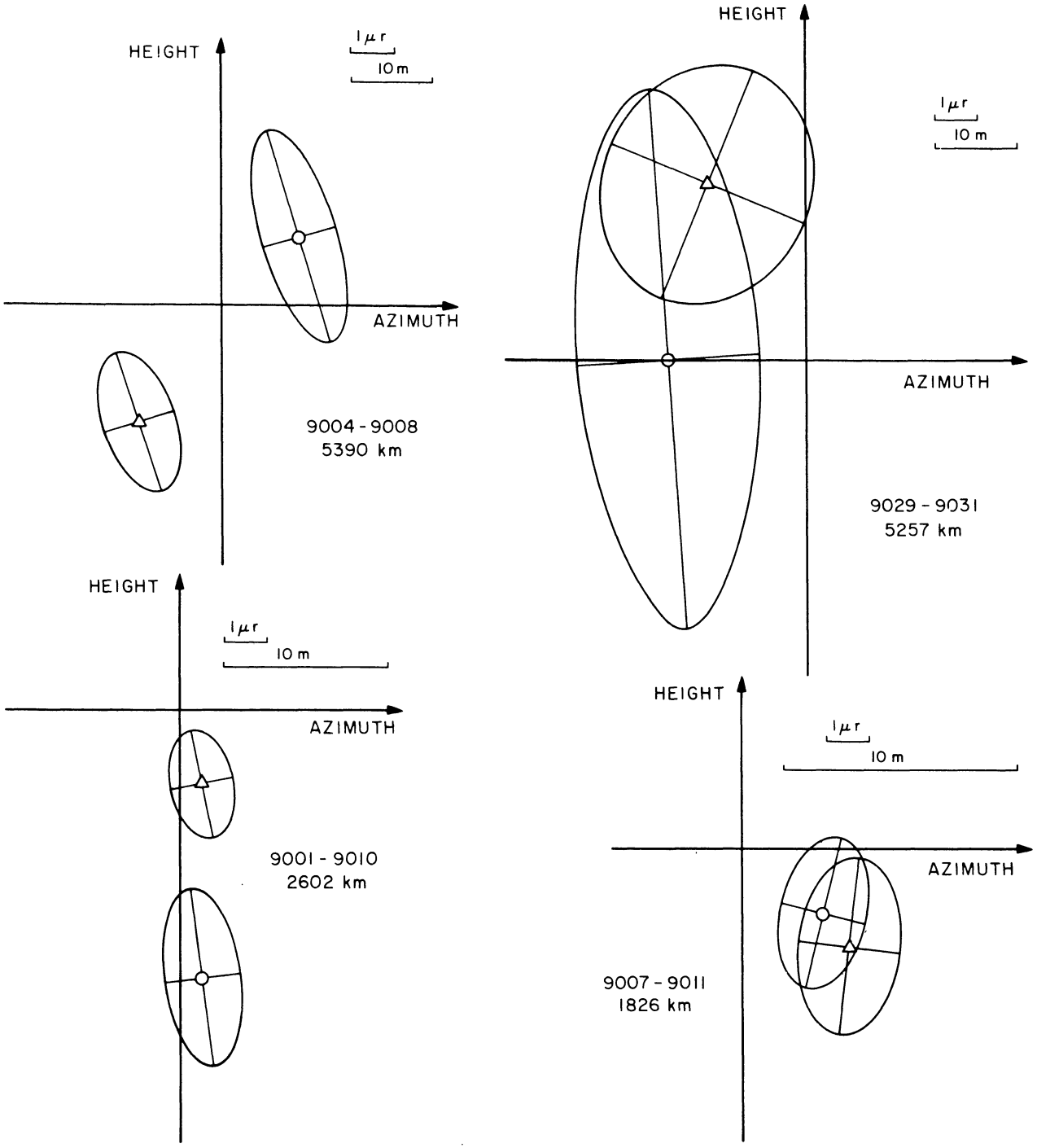

Fig. 4. Graphical representations of the station-station vector adjustment for four typical cases. The origin of the coordinate axes is the final combination solution. The results of phase 1 are denoted by O and the results of phase 3 by Δ. The error ellipses of the vectors have been projected onto a plane normal to these vectors.

These quantities are given in Table 7 and their values, averaged over the vectors used, indicate that this condition is not satisfied unless the variance estimates are multiplied by a factor

$$k^2 = \frac{\delta^2}{(1/2)(\sigma_1^2 + \sigma_2^2)} \quad .$$

The results in Table 7 yield a value of $k^2 = 2.8$, and the covariance matrix for the final geometric solution (phase 3 results) are multiplied by this number. Table 8 gives the directions between stations for which the number of simultaneously observed events was greater than 30.

TABLE 8. Direction cosines of the station-station vectors determined from the geometric solution. The accuracy components of these vectors refer to the right ascension – declination system.

Stations	ℓ	m	n	σ^2_δ	$\sigma^2_{\alpha-\theta}$	$\sigma_{\delta,\alpha-\theta}$
9001 9007	.5533023	-.1013373	-.8267934	.18	.10	-.04
9001 9009	.8673538	-.1488311	-.4749176	.10	.11	-.06
9001 9010	.9654355	-.1669484	-.2001563	.13	.14	-.07
9001 9012	-.7952945	.5590334	-.2344962	.31	.33	.21
9001 9113	-.8398599	.4984302	.2149481	1.39	1.13	.48
9001 9114	.1092630	.6856677	.7196676	1.09	.36	-.05
9002 9028	-.0386247	.3164774	.9478134	1.17	2.55	.64
9004 9008	-.3267909	.9374803	-.1197434	.28	.18	-.14
9004 9009	-.4414261	-.8138811	-.3778102	.65	.71	.52
9004 9010	-.6274856	-.7668075	-.1351590	.67	.72	.47
9004 9028	-.0379129	.8490291	-.5269841	.52	.37	-.04
9004 9029	.0149766	-.5736271	-.8189796	1.85	.90	.53
9004 9115	-.6890458	.3985935	.6052595	1.34	.89	-.35
9005 9006	.9152358	.3880030	-.1086147	.87	.69	.60
9005 9012	-.2473497	-.9394567	-.2371482	1.95	3.93	-2.22
9005 9117	-.3907658	-.8491967	-.3552001	3.84	4.00	-2.91
9006 9008	.9110447	-.4121793	.0102832	.82	.42	.33
9006 9028	.8289777	-.3212848	-.4577903	.60	.57	.23
9007 9009	.0984436	-.0040855	.9951342	.11	.24	.06
9007 9010	-.2021849	.0424031	.9784290	.10	.14	.05
9007 9011	.1850049	.4871397	-.8535034	.42	.26	.14
9007 9029	.7997396	.5301459	.2817124	.47	1.10	.13
9007 9031	-.0766869	.5210891	-.8500502	.98	.68	.11
9008 9115	-.0568170	-.8471905	.5282425	.83	.35	.21
9009 9010	-.6310606	.1066278	.7683704	.22	.39	.11
9009 9011	.0060328	.1892173	-.9819167	.17	.06	.03
9010 9114	-.5807342	.5531082	.5973434	.38	.33	.13
9012 9021	.7740228	-.5863195	.2389940	1.03	.49	-.24
9012 9114	.8019841	-.2028464	.5618495	.73	.64	.05
9012 9117	-.3703251	.8841371	-.2848876	2.24	1.98	1.23
9021 9113	-.6853701	.6053209	.4047893	6.55	6.69	.48
9028 9091	-.0872798	-.5447061	.8340728	1.54	.76	.03
9029 9031	-.6643697	-.0872145	-.7422982	.74	.94	-.09
9114 9113	-.5223312	-.5101533	-.6833109	1.27	1.05	.27

5. INFORMATION FROM DEEP-SPACE PROBES

The DSN has used data from its tracking of deep-space probes to obtain — among other parameters — the relative longitudes and the distances to the earth's axis of rotation of their antennas [Vegos and Trask, 1967; Trask and Vegos, 1968]. As the JPL sites can be related to nearby Baker-Nunn sites, by use of ground-survey information, a valuable and completely independent control of the results is possible. Comparison with the JPL data is particularly important for the two instances where the geometric solution is either very poor (South Africa) or nonexistent (Australia). The two sets of data also complement each other since the JPL solution gives a very strong scale and relative longitude determination but no latitude information, whereas the SAO solution accurately determines the orientation with respect to the astronomical reference system.

Comparisons of the JPL and SAO results were made by Veis [1966] and Vegos and Trask [1967] using data from the Ranger missions. However, more refined JPL solutions have recently become available using data from the Mariner 4 and 5 missions. The solution used in the present analysis is that of Mottinger [1969] called LS 25. Table 9 gives his determination for the station locations. Mottinger estimates the standard deviations of the computed quantities to be about 3 m. In this solution the polar-motion data from BIH and UT1 derived from USNO data are used. Thus, a difference in longitude between the JPL and the SAO solution can be expected. A longitude difference can also arise from possible discrepancies in the right-ascension definitions of the planetary ephemeris used by JPL and of the star catalog used at SAO.

The geodetic coordinates of the JPL and associated Baker-Nunn stations are given in Table 10. In three cases, 9002—4751 (South Africa), 9003—4741 (Australia), and 9113—4712 (United States), the survey distance between the

TABLE 9. Results for the locations of the JPL antennas as determined by Mottinger [1969].

Station	λ (deg)	r_s (km)	X (km)	Y (km)
4712	243.194559	5212.0535	-2350.4397	-4651.9819
4741	136.887507	5450.1986	-3978.7174	3724.8454
4742	148.981301	5205.3504	-4460.9809	2682.4097
4751	27.685432	5742.9417	5085.4425	2668.2678
4761	355.751007	4862.6078	4849.2429	- 360.2752

TABLE 10. Geodetic coordinates for the SAO and JPL stations.

Station	Datum	Geodetic Coordinates φ	Geodetic Coordinates λ	Height Mean Sea Level (m)	Height Ellipsoid (m)
9002	ARC	-25°57'33!'85	28°14'53!'91	1544	1544
4751	ARC	-25 53 21.16	27 41 08.52	1398	1405
9003	AND	-31 06 07.26	136 46 58.70	162	162
4741	AND	-31 22 59.36	136 53 10.16	153	152
4742	AND	-35 24 08.04	148 58 48.21	662	656
9004	EUR	36 27 51.37	353 47 42.09	26	-6
4761	EUR	40 25 47.72	355 45 08.28	788	769
9113	NAD	34 57 50.74	242 05 11.58	784	760
4712	NAD	35 17 59.85	243 11 43.41	989	967

stations is small and any datum tilts or distortions should not cause any problems when the geodetic survey information is used to relate the two earth-centered systems. However, for the other two JPL-SAO station groups 9003–4742 and 9004–4761, this may not be true.

In the case of the European datum the combined geometric-dynamic satellite solution gives the positions of nine stations that are also tied to the datum. Thus the relation, expressed by three translations, three rotations, and a scale [Lambeck, 1970], between these two coordinate systems can be determined and used to transform the geodetic coordinates of the stations 9004 and 4761 into the geocentric system. The "corrected" survey differences referring to this system can therefore be computed (Table 11). In the case of Australia, SAO has only one station tied to the datum and a complete datum orientation is not possible. However, a Naval Weapons Laboratory (NWL) Doppler solution by Anderle [1967] gives the geocentric coordinates for a number of stations that have also been tied to the Australian datum. Thus the corrected survey difference between 9003 and 4742 in the Anderle geocentric system can be computed in the same way as the European case. But it must be remembered that the Doppler solution describes a reference system different from the SAO system, and a further transformation (three rotations and a scale) is required to relate the geodetic coordinate difference to the SAO reference system. The longitude difference can be determined by a comparison of the coordinates obtained by SAO for their Baker-Nunn at 9023 with the coordinates obtained by NWL for a nearby Doppler site, but the other two rotation elements are indeterminate and are assumed to be zero. The scale difference is derived from the respective values of GM.

TABLE 11. Survey differences between the SAO and JPL stations. σ_H and σ_V are the accuracy estimates for the survey differences in horizontal coordinates and in the vertical component.

Stations	ΔX (km)	ΔY (km)	σ_H (m)	σ_V (m)
9002–4751	-29.331	48.258	1	1
9003–4741	-5.074	18.236	1	1
9003–4742	477.194	1060.673	6	1
9004–4761	256.347	194.932	3	1
9113–4712	-99.547	27.556	1	1

6. SURFACE-GRAVITY DATA

Surface-gravity data provide a means of comparing the satellite solution with an external standard and of improving the overall gravity-field solution. The satellite solutions are most suited for determining the lower order harmonics while the surface-gravity data are expected to contribute most to the higher order terms. The dynamic satellite solution described above gives a complete representation to degree and order 12, with the exception of the (11,7), (12,6), and (12,9) harmonics; and for higher degree only those coefficients with orders 1,2,3 and 12,13,14 have been determined from the present data. The surface gravity, on the other hand, does not reflect such a partiality to certain coefficients, and all terms of the same degree can be determined with about equal reliability.

The gravity anomalies Δg are related to the harmonic coefficients by

$$\Delta g = \gamma \sum_{\ell=2}^{\infty} \sum_{m=0}^{n} (\ell - 1)\left(\frac{a}{r}\right)^{\ell} (C_{\ell m} \cos m\lambda + S_{\ell m} \sin m\lambda)\, P_{\ell m}(\sin \phi) \quad ,$$

where $C_{2,0}$ and $C_{4,0}$ are referred to a specified reference ellipsoid, in this case 1/298.255, corresponding to Kozai's [1969] determination for J_2. Thus, if Δg is known all over the earth, the harmonic coefficients can be estimated. This approach was used by Köhnlein [1967b] and is also used here.

An alternative method of estimating the harmonics from the gravity data is by evaluating the following integral over the earth's surface (e.g., Kaula [1966a]):

$$\begin{Bmatrix} C_{\ell m} \\ S_{\ell m} \end{Bmatrix} = \frac{1}{4\pi\gamma(\ell - 1)} \iint_{\sigma} \Delta g\, P_{\ell m}(\sin \phi) \begin{Bmatrix} \cos m\lambda \\ \sin m\lambda \end{Bmatrix} d\sigma \quad .$$

According to Rapp [1969], there appear to be no differences of practical significance in these two formulations.

No serious attempt has been made to determine estimates of the zonal harmonics from the surface-gravity data because of its poor distribution, particularly at the southern latitudes. However, the data do contain some zonal information that has been filtered out before the analysis for the tesseral terms was made.

Data Used

Data prepared by Kaula [1966a] were used in this analysis. His basic data consisted of 1° × 1° mean free-air anomalies computed essentially by the techniques described by Uotila [1960]. These anomalies were combined to form mean values for areas of 60 × 60 ± 30 n mi (nautical miles) in order to obtain a set as nearly statistically uniform as possible. To obtain estimates for 300-n mi squares, Kaula next estimated 60-n mi area anomalies for the unsurveyed areas applying linear regression methods [Kaula, 1966c] to the 60-n mi means within the 300-n mi area. Finally, he computed the 300-n mi means as the arithmetic mean of all the observed and extrapolated 60-n mi means within the area. The results were 935 mean anomalies for 300-n mi squares covering 56.5% of the globe and are listed in Table 12.

For the remaining 43.5% of the globe three alternative assumptions were made in the present analysis:

1. No assumptions were made about these areas and only the observed anomalies were used.

2. The model anomalies generated by Kaula from a linear regression analysis of his 935 observed squares [Kaula, 1966d] were used.

3. The anomalies were set to zero and a large variance was used.

TABLE 12. 300 × 300 n mi mean free-air gravity anomalies according to Kaula [1966a]. The latitude φ and longitude λ refer to the middle of the square; n is the number of observed 60 × 60 n mi squares in each 300 × 300 n mi area.

φ	λ	Δg	n	φ	λ	Δg	n	φ	λ	Δg	n	φ	λ	Δg	n
87.5	60.0	0	9	87.5	180.0	9	11	87.5	300.0	10	9	82.5	20.0	23	10
82.5	60.0	9	3	82.5	100.0	-4	1	82.5	180.0	3	3	82.5	220.0	9	6
82.5	260.0	6	1	82.5	300.0	-14	1	82.5	340.0	19	1	77.5	11.5	12	12
77.5	34.0	8	2	77.5	56.5	3	1	77.5	146.5	-14	2	77.5	281.5	7	2
77.5	304.0	17	4	77.5	349.0	30	7	72.5	24.5	18	4	72.5	41.0	11	1
72.5	57.0	3	5	72.5	73.5	3	2	72.5	90.0	-5	5	72.5	106.5	-5	11
72.5	123.0	8	2	72.5	188.0	-3	1	72.5	204.5	-6	2	72.5	221.0	3	3
72.5	237.0	-10	2	72.5	253.5	12	1	72.5	270.0	-2	2	72.5	286.5	-17	2
72.5	303.0	9	9	72.5	319.0	31	8	72.5	335.5	16	9	72.5	352.0	15	2
67.5	6.5	22	4	67.5	19.5	5	25	67.5	32.5	11	4	67.5	45.0	14	7
67.5	57.5	-7	9	67.5	70.5	-19	1	67.5	83.5	9	9	67.5	109.5	4	2
67.5	186.5	1	4	67.5	199.5	13	10	67.5	212.5	33	4	67.5	225.0	8	7
67.5	237.5	-11	2	67.5	250.5	-15	2	67.5	289.5	9	2	67.5	302.5	-6	4
67.5	315.0	4	4	67.5	327.5	22	1	67.5	340.5	35	4	62.5	5.5	22	18
62.5	16.5	-5	25	62.5	27.5	0	25	62.5	38.5	7	25	62.5	49.5	4	22
62.5	60.0	-4	5	62.5	70.5	-22	3	62.5	81.5	0	5	62.5	190.5	9	17
62.5	201.5	23	17	62.5	212.5	37	20	62.5	223.5	28	17	62.5	234.5	-5	4
62.5	245.5	-11	3	62.5	289.5	-2	5	62.5	310.5	-25	3	62.5	332.5	25	3
62.5	343.5	32	9	62.5	354.5	7	4	57.5	4.5	7	9	57.5	13.5	6	25
57.5	23.0	-9	24	57.5	32.5	6	24	57.5	41.5	9	24	57.5	50.5	12	19
57.5	60.0	13	24	57.5	69.5	-3	15	57.5	78.5	-3	24	57.5	87.5	-2	8
57.5	97.0	-26	4	57.5	106.5	-25	1	57.5	115.5	3	4	57.5	180.0	-4	2
57.5	189.5	16	15	57.5	198.5	32	9	57.5	207.5	22	15	57.5	217.0	7	9
57.5	226.5	8	15	57.5	235.5	5	10	57.5	244.5	-8	15	57.5	253.5	-9	23
57.5	263.0	-14	18	57.5	272.5	-10	1	57.5	290.5	-10	18	57.5	337.0	-9	5
57.5	346.5	7	8	57.5	355.5	16	20	52.5	4.0	0	8	52.5	12.0	14	25
52.5	20.5	7	25	52.5	29.0	9	25	52.5	37.0	12	25	52.5	45.0	8	25
52.5	53.0	1	25	52.5	61.0	9	25	52.5	69.5	4	25	52.5	78.0	-15	24
52.5	86.0	-3	21	52.5	94.0	7	4	52.5	102.0	-14	21	52.5	110.5	-8	8
52.5	119.0	10	4	52.5	127.0	7	9	52.5	143.0	-3	4	52.5	184.0	-34	16
52.5	192.0	-4	15	52.5	200.5	-27	8	52.5	209.0	-3	15	52.5	217.0	3	1
52.5	225.0	-12	10	52.5	233.0	-15	6	52.5	241.0	11	10	52.5	249.5	0	25
52.5	258.0	8	25	52.5	266.0	-2	25	52.5	274.0	-17	25	52.5	282.0	-16	10
52.5	290.5	-7	2	52.5	299.0	-11	1	52.5	323.0	12	2	52.5	331.0	21	7
52.5	339.5	3	2	52.5	348.0	20	6	52.5	356.0	17	2	47.5	3.5	9	25
47.5	11.0	7	25	47.5	11.0	7	23	47.5	18.5	27	25	47.5	25.5	33	24
47.5	33.0	12	22	47.5	40.5	4	16	47.5	47.5	-13	22	47.5	55.0	-15	25
47.5	62.5	-11	25	47.5	69.5	-13	24	47.5	77.0	-14	25	47.5	84.5	-21	5
47.5	114.0	6	14	47.5	121.5	12	16	47.5	128.5	12	14	47.5	136.0	13	2
47.5	143.5	-10	5	47.5	187.5	15	5	47.5	194.5	16	5	47.5	202.0	11	4
47.5	209.5	1	5	47.5	216.5	-7	1	47.5	224.0	-6	5	47.5	231.5	-12	24
47.5	238.5	1	25	47.5	246.0	22	25	47.5	253.5	24	25	47.5	260.5	14	25
47.5	268.0	6	24	47.5	275.5	-12	25	47.5	283.0	-12	24	47.5	290.5	-9	14
47.5	297.5	2	9	47.5	305.0	12	2	47.5	319.5	10	9	47.5	327.0	6	5
47.5	334.5	34	11	47.5	341.5	24	21	47.5	349.0	9	11	47.5	356.5	8	24
42.5	3.5	20	25	42.5	10.5	6	16	42.5	17.0	34	25	42.5	23.5	29	10
42.5	30.5	3	10	42.5	37.5	9	23	42.5	44.5	24	10	42.5	51.0	-36	25
42.5	57.5	-2	25	42.5	64.5	-12	23	42.5	71.5	-35	25	42.5	78.5	-32	2
42.5	85.0	28	6	42.5	91.5	-26	2	42.5	112.0	-8	6	42.5	118.5	-1	18
42.5	125.5	7	5	42.5	132.5	9	10	42.5	139.5	31	5	42.5	146.0	3	2
42.5	186.5	-5	3	42.5	193.5	-8	5	42.5	207.5	1	3	42.5	214.0	-1	6
42.5	220.5	-13	10	42.5	227.5	-14	22	42.5	234.5	-2	10	42.5	241.5	17	25
42.5	248.0	24	25	42.5	254.5	22	25	42.5	261.5	4	25	42.5	268.5	-7	25
42.5	275.0	-7	25	42.5	281.5	-8	24	42.5	288.5	6	25	42.5	295.5	-7	11
42.5	302.5	-24	12	42.5	309.0	4	7	42.5	315.5	13	12	42.5	322.5	19	6
42.5	329.5	21	11	42.5	336.5	22	16	42.5	343.0	10	11	42.5	349.5	17	23
42.5	356.5	22	25	37.5	3.0	17	24	37.5	9.5	19	25	37.5	16.0	6	15
37.5	22.0	-23	12	37.5	28.5	5	10	37.5	35.0	27	12	37.5	41.0	33	11
37.5	47.5	44	9	37.5	54.0	-6	18	37.5	60.0	-8	9	37.5	66.0	-29	15
37.5	72.5	2	10	37.5	79.0	4	2	37.5	85.0	-15	10	37.5	110.5	-2	9
37.5	117.0	-21	5	37.5	123.0	7	9	37.5	129.5	20	5	37.5	136.0	35	22
37.5	142.0	24	1	37.5	148.5	12	1	37.5	174.0	3	1	37.5	180.0	0	4

TABLE 12 (Cont.)

ϕ	λ	Δg	n	ϕ	λ	Δg	n	ϕ	λ	Δg	n	ϕ	λ	Δg	n
37.5	192.5	-10	2	37.5	211.5	-4	8	37.5	218.0	-13	2	37.5	224.0	-17	7
37.5	230.5	-18	24	37.5	237.0	-16	25	37.5	243.0	3	24	37.5	249.5	11	24
37.5	256.0	18	25	37.5	262.0	-8	25	37.5	268.5	-4	25	37.5	275.0	-1	25
37.5	281.0	4	23	37.5	287.5	-20	17	37.5	294.0	-18	23	37.5	300.0	-15	4
37.5	306.0	-7	6	37.5	312.5	-6	5	37.5	319.0	10	6	37.5	325.0	29	17
37.5	331.5	37	13	37.5	338.0	9	16	37.5	344.0	10	13	37.5	350.5	3	24
37.5	357.0	13	16	32.5	3.0	17	14	32.5	9.0	-1	16	32.5	15.0	2	4
32.5	21.0	-29	17	32.5	27.0	-39	21	32.5	32.5	-16	17	32.5	38.0	36	2
32.5	44.0	2	10	32.5	50.0	26	2	32.5	56.0	4	10	32.5	62.0	3	7
32.5	68.0	-4	20	32.5	74.0	-37	5	32.5	80.0	49	20	32.5	86.0	6	8
32.5	109.0	-25	15	32.5	115.0	-23	9	32.5	121.0	4	15	32.5	127.0	21	16
32.5	133.0	22	21	32.5	139.0	14	14	32.5	145.0	-26	21	32.5	150.5	-7	8
32.5	156.0	-7	5	32.5	162.0	-19	4	32.5	168.0	-12	5	32.5	174.0	-8	5
32.5	180.0	-6	3	32.5	186.0	-8	3	32.5	198.0	-5	3	32.5	209.5	2	1
32.5	215.0	-3	1	32.5	221.0	-3	9	32.5	227.0	-13	1	32.5	233.0	-20	21
32.5	239.0	-24	20	32.5	245.0	-1	22	32.5	251.0	-1	20	32.5	257.0	5	25
32.5	263.0	-6	25	32.5	268.5	2	25	32.5	274.0	1	25	32.5	280.0	-1	17
32.5	286.0	-37	19	32.5	292.0	-26	17	32.5	298.0	-5	19	32.5	304.0	-4	3
32.5	310.0	-6	5	32.5	316.0	15	7	32.5	322.0	17	5	32.5	327.5	22	2
32.5	333.0	10	4	32.5	339.0	2	11	32.5	345.0	3	4	32.5	351.0	40	22
32.5	357.0	42	13	27.5	3.0	-4	1	27.5	8.5	-6	13	27.5	31.0	7	8
27.5	36.5	-1	4	27.5	42.0	2	19	27.5	48.0	-15	4	27.5	53.5	-34	6
27.5	59.0	30	20	27.5	65.0	-4	18	27.5	70.5	-10	20	27.5	76.0	-14	15
27.5	81.5	-80	12	27.5	87.0	-31	11	27.5	93.0	-45	12	27.5	98.5	-12	9
27.5	104.0	-3	14	27.5	110.0	-6	10	27.5	115.5	0	14	27.5	121.0	0	8
27.5	126.5	26	1	27.5	132.0	-13	3	27.5	138.0	13	1	27.5	143.5	-16	4
27.5	160.5	-8	4	27.5	166.0	-17	5	27.5	171.5	-17	4	27.5	177.0	-10	21
27.5	183.0	-16	5	27.5	188.5	-3	7	27.5	194.0	8	5	27.5	200.0	15	6
27.5	205.5	0	3	27.5	211.0	3	7	27.5	216.5	4	3	27.5	222.0	-4	6
27.5	228.0	-18	1	27.5	233.5	-6	9	27.5	239.0	-24	1	27.5	245.0	-17	8
27.5	250.5	-11	17	27.5	256.0	19	21	27.5	261.5	-4	17	27.5	267.0	9	16
27.5	273.0	-9	20	27.5	278.5	2	24	27.5	284.0	-26	20	27.5	290.0	-33	10
27.5	295.5	-18	9	27.5	301.0	-24	6	27.5	306.5	-17	9	27.5	312.0	7	3
27.5	318.0	17	1	27.5	323.5	-4	2	27.5	329.0	-5	1	27.5	335.0	-11	7
27.5	340.5	7	6	27.5	346.0	20	2	27.5	351.5	24	6	27.5	357.0	7	12
22.5	2.5	27	7	22.5	8.0	33	1	22.5	29.5	0	7	22.5	35.0	-7	5
22.5	40.5	21	5	22.5	45.5	-12	21	22.5	51.0	-31	5	22.5	67.0	6	19
22.5	72.5	5	23	22.5	78.0	7	17	22.5	83.5	-6	23	22.5	88.5	-10	22
22.5	94.0	-18	11	22.5	99.5	-12	13	22.5	104.5	-24	11	22.5	110.0	-8	9
22.5	115.5	3	10	22.5	121.0	-4	4	22.5	126.5	-10	10	22.5	142.5	10	5
22.5	164.0	-14	4	22.5	169.5	-8	5	22.5	180.0	-9	4	22.5	185.5	-6	6
22.5	190.5	4	9	22.5	196.0	24	10	22.5	201.5	27	9	22.5	207.0	-5	10
22.5	212.5	-11	12	22.5	217.5	-7	10	22.5	223.0	-9	12	22.5	228.5	-11	5
22.5	233.5	-11	1	22.5	244.5	-3	6	22.5	250.0	-9	1	22.5	255.5	15	21
22.5	260.5	15	7	22.5	271.5	16	13	22.5	276.5	-6	7	22.5	282.0	-6	23
22.5	287.5	-60	12	22.5	293.0	-25	5	22.5	298.5	-6	12	22.5	303.5	-18	9
22.5	309.0	-13	6	22.5	314.5	-3	5	22.5	319.5	-6	6	22.5	325.0	-6	3
22.5	330.5	-6	1	22.5	336.0	-3	8	22.5	341.5	-1	1	22.5	346.5	18	3
22.5	352.0	-11	16	22.5	357.5	-10	21	17.5	2.5	5	16	17.5	7.5	6	1
17.5	18.5	-4	7	17.5	34.0	8	8	17.5	39.5	5	7	17.5	44.5	-1	12
17.5	49.5	-23	2	17.5	54.5	-11	2	17.5	70.5	5	2	17.5	75.5	-29	13
17.5	80.5	-18	4	17.5	86.0	12	16	17.5	96.5	-3	4	17.5	101.5	-16	13
17.5	107.0	-18	1	17.5	112.5	3	1	17.5	117.5	22	1	17.5	122.5	34	4
17.5	127.5	4	5	17.5	143.5	22	13	17.5	164.5	-12	5	17.5	169.5	-8	6
17.5	174.5	-1	5	17.5	180.0	-4	3	17.5	185.5	5	5	17.5	190.5	11	5
17.5	195.5	-1	3	17.5	200.5	2	1	17.5	206.0	62	3	17.5	227.0	-6	4
17.5	232.5	-15	5	17.5	237.5	-13	5	17.5	242.5	-13	5	17.5	247.5	-10	7
17.5	253.0	-2	17	17.5	258.5	-3	10	17.5	263.5	6	17	17.5	268.5	9	8
17.5	274.0	34	9	17.5	279.5	-8	13	17.5	284.5	-23	9	17.5	289.5	11	17
17.5	294.5	-48	10	17.5	300.0	-37	8	17.5	305.5	-24	10	17.5	310.5	-22	11
17.5	315.5	-19	9	17.5	320.5	-23	7	17.5	326.0	-9	9	17.5	331.5	4	6
17.5	336.5	10	6	17.5	341.5	9	14	17.5	347.0	14	6	17.5	352.5	0	20
17.5	357.5	12	22	12.5	2.5	0	12	12.5	7.5	8	22	12.5	12.5	31	2

TABLE 12 (Cont.)

φ	λ	Δg	n	φ	λ	Δg	n	φ	λ	Δg	n	φ	λ	Δg	n
12.5	18.0	-3	2	12.5	23.5	5	1	12.5	28.5	3	2	12.5	33.5	-3	4
12.5	38.5	9	8	12.5	43.5	4	4	12.5	48.5	-4	8	12.5	54.0	1	11
12.5	74.5	-30	15	12.5	79.5	-24	1	12.5	90.0	-9	15	12.5	95.5	0	19
12.5	100.5	-4	17	12.5	105.5	-7	7	12.5	110.5	-4	17	12.5	120.5	29	13
12.5	126.0	8	1	12.5	131.5	14	2	12.5	136.5	-11	1	12.5	141.5	-3	12
12.5	146.5	-25	6	12.5	151.5	2	5	12.5	156.5	-10	6	12.5	162.0	-12	6
12.5	167.5	-2	6	12.5	192.5	-5	4	12.5	198.0	6	6	12.5	249.5	7	8
12.5	254.5	-9	6	12.5	259.5	5	11	12.5	264.5	9	6	12.5	270.0	9	9
12.5	275.5	32	10	12.5	280.5	-11	18	12.5	285.5	-18	10	12.5	290.5	-38	19
12.5	295.5	-29	23	12.5	300.5	-36	21	12.5	306.0	-36	23	12.5	311.5	-39	9
12.5	316.5	-15	5	12.5	321.5	-17	8	12.5	326.5	-16	5	12.5	331.5	-13	9
12.5	336.5	-9	12	12.5	342.0	9	14	12.5	347.5	16	12	12.5	352.5	9	23
12.5	357.5	9	15	7.5	2.5	23	11	7.5	7.5	8	15	7.5	12.5	19	2
7.5	17.5	-3	2	7.5	22.5	-7	4	7.5	38.0	12	2	7.5	43.5	6	2
7.5	63.5	-11	3	7.5	68.5	-26	5	7.5	73.5	-5	3	7.5	78.5	-22	3
7.5	83.5	6	1	7.5	88.5	-9	4	7.5	93.5	-34	1	7.5	98.5	3	3
7.5	103.5	-2	2	7.5	114.5	2	4	7.5	119.5	9	2	7.5	124.5	39	4
7.5	129.5	-15	7	7.5	134.5	23	2	7.5	139.5	9	7	7.5	144.5	14	3
7.5	149.5	26	4	7.5	159.5	20	6	7.5	164.5	4	4	7.5	169.5	23	3
7.5	185.5	-15	7	7.5	190.5	-5	1	7.5	195.5	0	7	7.5	251.0	-12	1
7.5	256.5	-1	1	7.5	266.5	0	12	7.5	271.5	12	1	7.5	276.5	16	18
7.5	281.5	27	23	7.5	286.5	20	20	7.5	291.5	11	23	7.5	296.5	1	13
7.5	301.5	-9	16	7.5	306.5	-24	21	7.5	311.5	-38	16	7.5	316.5	-34	13
7.5	322.0	-9	7	7.5	327.5	2	10	7.5	332.5	2	7	7.5	337.5	5	8
7.5	342.5	8	3	7.5	347.5	24	19	7.5	352.5	28	3	7.5	357.5	18	8
2.5	7.5	2	4	2.5	12.5	13	7	2.5	17.5	-9	4	2.5	22.5	-26	10
2.5	27.5	2	14	2.5	32.5	-7	4	2.5	37.5	-10	14	2.5	77.5	-14	6
2.5	92.5	-5	10	2.5	97.5	17	12	2.5	102.5	18	10	2.5	107.5	14	8
2.5	112.5	21	15	2.5	117.5	27	15	2.5	122.5	36	15	2.5	127.5	23	4
2.5	132.5	34	2	2.5	142.5	1	1	2.5	147.5	0	2	2.5	152.5	-2	6
2.5	182.5	-2	5	2.5	187.5	-8	2	2.5	272.5	-1	5	2.5	277.5	-1	23
2.5	282.5	27	13	2.5	287.5	22	1	2.5	292.5	4	13	2.5	297.5	7	1
2.5	302.5	-6	5	2.5	307.5	-11	10	2.5	312.5	-14	5	2.5	317.5	-19	19
2.5	322.5	-9	18	2.5	327.5	1	10	2.5	332.5	8	18	2.5	337.5	-2	8
2.5	342.5	-9	1	2.5	347.5	-10	3	2.5	352.5	11	1	-2.5	7.5	9	5
-2.5	12.5	-7	18	-2.5	17.5	-22	25	-2.5	22.5	-37	18	-2.5	27.5	9	7
-2.5	32.5	-14	14	-2.5	37.5	29	1	-2.5	42.5	-12	14	-2.5	72.5	-14	1
-2.5	77.5	-18	1	-2.5	92.5	6	5	-2.5	97.5	2	1	-2.5	102.5	25	14
-2.5	107.5	34	10	-2.5	112.5	29	21	-2.5	117.5	24	10	-2.5	122.5	-7	18
-2.5	127.5	6	22	-2.5	132.5	20	11	-2.5	137.5	11	22	-2.5	142.5	-14	2
-2.5	147.5	30	5	-2.5	152.5	-7	5	-2.5	177.5	-17	5	-2.5	182.5	-8	4
-2.5	187.5	-7	7	-2.5	277.5	-6	13	-2.5	282.5	6	7	-2.5	287.5	25	1
-2.5	297.5	-5	2	-2.5	302.5	-13	2	-2.5	307.5	-5	2	-2.5	312.5	-12	9
-2.5	317.5	-24	18	-2.5	322.5	-5	10	-2.5	327.5	-4	18	-2.5	332.5	-7	14
-2.5	337.5	-12	13	-2.5	342.5	-4	6	-2.5	347.5	3	13	-2.5	352.5	6	2
-7.5	12.5	11	2	-7.5	17.5	-1	12	-7.5	22.5	-3	2	-7.5	27.5	-3	14
-7.5	32.5	0	12	-7.5	38.0	7	1	-7.5	68.5	-3	12	-7.5	73.5	24	4
-7.5	98.5	-3	8	-7.5	103.5	-4	19	-7.5	109.0	23	8	-7.5	114.5	24	16
-7.5	119.5	-4	17	-7.5	124.5	17	17	-7.5	129.5	-25	17	-7.5	134.5	-8	4
-7.5	139.5	4	4	-7.5	149.5	-69	8	-7.5	154.5	-21	4	-7.5	159.5	43	1
-7.5	169.5	-1	6	-7.5	174.5	-10	3	-7.5	180.0	-2	6	-7.5	185.5	-7	1
-7.5	200.5	17	1	-7.5	210.5	14	1	-7.5	220.5	17	1	-7.5	276.5	-10	4
-7.5	281.5	-7	7	-7.5	286.5	-7	5	-7.5	311.5	-17	7	-7.5	316.5	-23	8
-7.5	322.0	9	10	-7.5	327.5	-25	6	-7.5	332.5	-10	10	-7.5	337.5	-10	17
-7.5	342.5	-2	20	-7.5	347.5	1	2	-7.5	352.5	-4	20	-7.5	357.5	-7	1
-12.5	12.5	7	2	-12.5	28.5	8	1	-12.5	33.5	3	2	-12.5	38.5	6	5
-12.5	48.5	13	2	-12.5	64.5	-8	2	-12.5	69.5	0	2	-12.5	100.5	6	2
-12.5	105.5	13	4	-12.5	110.5	-1	8	-12.5	115.5	-14	4	-12.5	120.5	-16	4
-12.5	126.0	-2	12	-12.5	131.5	29	3	-12.5	136.5	15	12	-12.5	141.5	18	1
-12.5	146.5	14	4	-12.5	156.5	21	2	-12.5	162.0	25	4	-12.5	167.5	14	1
-12.5	172.5	-10	3	-12.5	177.5	1	2	-12.5	182.5	9	3	-12.5	187.5	3	1
-12.5	208.5	16	6	-12.5	280.5	-16	6	-12.5	285.5	22	6	-12.5	290.5	39	6
-12.5	295.5	38	3	-12.5	311.5	3	4	-12.5	316.5	1	3	-12.5	321.5	18	4

TABLE 12 (Cont.)

φ	λ	Δg	n	φ	λ	Δg	n	φ	λ	Δg	n	φ	λ	Δg	n
-12.5	326.5	-21	5	-12.5	342.0	-3	9	-12.5	347.5	-6	5	-12.5	352.5	-3	3
-12.5	357.5	-2	1	-17.5	2.5	6	3	-17.5	7.5	18	1	-17.5	13.0	3	1
-17.5	18.5	9	2	-17.5	23.5	5	3	-17.5	28.5	18	2	-17.5	34.0	11	13
-17.5	44.5	-1	11	-17.5	49.5	17	3	-17.5	60.0	16	11	-17.5	112.5	-19	9
-17.5	122.5	13	11	-17.5	127.5	21	5	-17.5	133.0	-3	11	-17.5	138.5	4	20
-17.5	143.5	17	6	-17.5	148.5	1	5	-17.5	154.0	8	6	-17.5	159.5	-1	1
-17.5	164.5	4	3	-17.5	169.5	53	5	-17.5	174.5	26	3	-17.5	180.0	6	3
-17.5	284.5	3	10	-17.5	289.5	44	9	-17.5	294.5	71	10	-17.5	300.0	19	4
-17.5	310.5	-13	3	-17.5	315.5	-11	6	-17.5	320.5	-35	3	-17.5	352.5	42	2
-22.5	2.5	13	2	-22.5	8.0	12	1	-22.5	13.5	4	2	-22.5	18.5	8	4
-22.5	24.0	-3	20	-22.5	29.5	4	5	-22.5	35.0	-14	20	-22.5	45.5	21	6
-22.5	51.0	9	8	-22.5	56.5	22	4	-22.5	110.0	-6	8	-22.5	115.5	12	17
-22.5	121.0	8	14	-22.5	126.5	-4	5	-22.5	131.5	-4	14	-22.5	137.0	9	18
-22.5	142.5	3	25	-22.5	147.5	24	5	-22.5	153.0	11	25	-22.5	158.5	7	9
-22.5	164.0	47	7	-22.5	169.5	20	7	-22.5	174.5	33	7	-22.5	180.0	8	10
-22.5	185.5	5	8	-22.5	287.5	2	10	-22.5	293.0	45	8	-22.5	298.5	-12	1
-22.5	303.5	-5	1	-22.5	309.0	-11	6	-22.5	314.5	3	1	-22.5	319.5	-16	2
-27.5	14.0	18	16	-27.5	20.0	13	25	-27.5	25.5	9	16	-27.5	31.0	31	5
-27.5	36.5	0	6	-27.5	42.0	9	4	-27.5	48.0	-1	6	-27.5	59.0	3	5
-27.5	65.0	10	3	-27.5	70.5	18	1	-27.5	110.0	11	3	-27.5	115.5	5	11
-27.5	121.0	12	1	-27.5	126.5	1	9	-27.5	132.0	-10	1	-27.5	138.0	-5	14
-27.5	143.5	-1	21	-27.5	149.0	17	10	-27.5	155.0	12	21	-27.5	160.5	11	4
-27.5	166.0	19	2	-27.5	171.5	8	3	-27.5	177.0	-1	2	-27.5	183.0	24	6
-27.5	290.0	41	14	-27.5	295.5	2	11	-27.5	301.0	15	14	-27.5	306.5	-8	3
-27.5	312.0	-4	2	-27.5	318.0	-20	6	-32.5	3.0	15	2	-32.5	9.0	5	7
-32.5	15.0	5	25	-32.5	21.0	21	20	-32.5	27.0	16	25	-32.5	32.5	2	1
-32.5	74.0	4	1	-32.5	91.5	16	3	-32.5	109.0	-8	1	-32.5	115.0	-14	8
-32.5	121.0	-12	10	-32.5	127.0	-21	10	-32.5	133.0	-13	10	-32.5	139.0	9	19
-32.5	145.0	6	21	-32.5	150.5	26	4	-32.5	156.0	-5	21	-32.5	162.0	-3	5
-32.5	180.0	-8	4	-32.5	186.0	-13	7	-32.5	286.0	-3	4	-32.5	292.0	12	21
-32.5	298.0	13	3	-32.5	304.0	8	2	-32.5	310.0	2	3	-32.5	322.0	-2	3
-32.5	327.5	-9	3	-32.5	333.0	8	1	-32.5	339.0	8	3	-32.5	351.0	-4	4
-32.5	357.0	13	1	-37.5	22.0	-6	4	-37.5	28.5	1	1	-37.5	142.0	9	13
-37.5	148.5	18	4	-37.5	155.0	-3	5	-37.5	161.0	-8	4	-37.5	167.5	9	15
-37.5	174.0	26	15	-37.5	180.0	5	1	-37.5	281.0	3	15	-37.5	287.5	20	12
-37.5	294.0	5	19	-37.5	300.0	14	3	-37.5	306.0	0	19	-37.5	312.5	-7	2
-37.5	338.0	12	3	-37.5	350.5	8	2	-42.5	166.5	-7	3	-42.5	173.5	6	1
-42.5	180.0	0	3	-42.5	281.5	1	2	-42.5	288.5	14	3	-42.5	295.5	3	2
-47.5	69.5	8	4	-47.5	165.5	20	3	-47.5	172.5	17	4	-47.5	283.0	-25	7
-47.5	290.5	2	1	-52.5	159.5	34	1	-52.5	168.0	12	1	-52.5	282.0	6	12
-52.5	290.5	1	2	-52.5	299.0	-5	3	-57.5	290.5	19	2	-62.5	300.0	22	4
-67.5	32.5	25	1	-67.5	45.0	9	1	-67.5	135.0	0	1	-67.5	147.5	6	1
-67.5	276.5	6	1	-67.5	289.5	20	2	-72.5	172.0	7	1	-77.5	169.0	15	4
-77.5	191.5	-2	6	-77.5	214.0	-10	9	-77.5	236.5	-1	6	-77.5	259.0	-14	3
-77.5	281.5	14	3	-77.5	304.0	2	5	-77.5	326.5	-17	3	-82.5	260.0	4	7
-82.5	300.0	-16	5	-87.5	60.0	-17	5	-87.5	180.0	-17	5				

Kaula used for the variance of each 300-n mi square

$$\sigma^2_{g_i} = g_T^2/(n_i + 1) \quad ,$$

where $g_T^2 = 274$ mgal^2 is the mean value of the square of the gravity anomaly, and n is the number of observed 60-n mi areas contained in the 300-n mi square.

However, the several assumptions made in computing the gravity anomaly by linear regression may make this variance too small. For example, for the observed squares $g_T^2 = 274$ mgal^2, but the corresponding number for the model anomalies is only 121 mgal^2. The most important assumption made is the one restricting the regression analysis to points within the 300-n mi square and ignoring possible correlations of gravity with topography. Consequently, in the present analysis the above variance estimates have been multiplied by a factor of 4. In the analyses of earlier iterations of the combination solution this factor was found to give a set of potential coefficients that improved both the satellite orbits and the surface-gravity comparison. With this variance a 300-n mi square with a surveyed 60-n mi area receives a standard deviation of 23 mgal, while a completely surveyed 300-n mi area (twenty-five 60-n mi squares) receives a standard deviation of 6.5 mgal.

Some screening of the surface-gravity data was done by comparing the gravity anomalies from the combination solution in any one iteration with the surface-gravity data and rejecting any anomaly that differed from the satellite-computed one by more than about three times the square root of the mean square difference of the two data sets. This does not necessarily imply an error in the surface-gravity data, but could mean that the rejected anomaly represents a short-wavelength variation that is not reflected in the satellite solution.

In the final solution, 38 anomalies were rejected. Of these, five were squares with $n \geq 10$ and one was a square with $n \geq 20$.

More recent surface-gravity compilations have been published by Talwani and Le Pichon [1969] and Le Pichon and Talwani [1969] for the Atlantic and Indian oceans. These new data have been used for comparisons with the new satellite combination solutions given here.

A comparison of results obtained using the different assumptions about the surface gravity in the unsurveyed areas indicates no difference between the anomaly set derived from regression analysis and the set of zero anomalies. This may have been expected since g_T^2 for the predicted anomalies is only 121 $mgal^2$, very much less than either the $g_T^2 = 274$ $mgal^2$ for the observed squares and the variances associated with the predicted values $(30\ mgal)^2$.

However, these two tests did show a difference in results from the one that ignored the unsurveyed areas altogether. This difference occurred in those extensive areas in southern latitudes where there were no surface data and where, because of the unfavorable station distribution, a direct observation of the acceleration of the satellite is not possible. The effect of using the model anomalies was to reduce by about 5 m the heights of the major geoid features in these areas. In the other areas the differences in geoid heights did not exceed 2 m.

7. COMPARISONS AND COMBINATION SOLUTION

Data from various sources can be combined to determine geodetic parameters of the earth. For example, both the dynamic and the geometric methods of satellite geodesy provide station-position information. The former method, in addition, yields information on the earth's potential or gravity — parameters that can also be estimated from surface-gravity measurements. The DSN tracking of deep-space flights provides estimates of GM and some of the station-position components, while astrogeodetic leveling and terrestrial triangulation also furnish geoid and relative station-position information.

All four methods of estimating geodetic parameters discussed in the preceding sections are incomplete in one way or another, and inadequacies in the mathematical models used often lead to unrealistic accuracy estimates. Consequently, the data from the different sources serve two purposes: one of comparison, to obtain realistic accuracy estimates and to resolve any biases in the results; and one of combination, to obtain the most complete and reliable set of geodetic parameters.

Combination Solution

In combining the two satellite solutions it must be remembered that the geometric solution is essentially unscaled and its origin is arbitrarily determined, so that in the transformation linking it to the dynamic solution three translation and one scale parameters must be introduced. A rotation term is also introduced to determine whether a systematic longitude discrepancy exists between these two solutions. Such a term could conceivably arise from correlations that exist in the dynamic solution among longitude, time, and right ascension of the node.

The JPL solution of Mottinger [1969] is combined with the satellite solution by introducing a second longitude rotation and a second scale parameter. The need for the former has been discussed in Section 5, and the latter was introduced to absorb possible biases in either solution that have the characteristic of a scale error. In theory, this scale factor should be zero since both SAO and JPL have used the same value for GM, but "pseudo" scale errors could be introduced. For example, a systematic error in the refraction corrections to Baker-Nunn observations could have an effect similar to a scale error.

In combining the JPL solution with the other data, the normalized covariance matrix supplied by Mottinger was used. This matrix was scaled by his accuracy estimates for the components of the station positions and preserves the strong correlation that exists between the longitudes of the solution.

The results from the surface-gravity analysis can be directly related to the combined solution since both refer to the same reference ellipsoid and GM. The zonal harmonics derived by Kozai have not been included in this combination, since his solution is quite independent of the satellite analysis of the tesseral harmonics, and the surface-gravity data, because of their poor distribution, do not contain any significant zonal information.

The final combination solution contains a total of 424 unknowns, 117 station coordinates, 296 harmonic coefficients, and 11 scale, rotation, and translation parameters. In a solution of this kind several iterations were made (as described in Section 3) and several alternative weighting schemes considered. These weight factors are used to scale the covariance matrices derived for the individual solutions and used in the combination. As already indicated, the covariance matrix of the geometric solution results has been multiplied by 2.8 and the covariance matrix of the surface-gravity results by 4.0. The covariance matrix of the dynamical solution results has been multiplied by 4.5 for the reasons described in the next section, while for the JPL results, the accuracy estimates of Mottinger have been adopted without any further modification. This weighting scheme gives the best

agreement in the tests described in the next section. The final results for station coordinates are presented in Table 13 and for harmonic coefficients in Table 14.

Table 13. Geocentric coordinates (in Mm) of the stations determined in the final combination solution. The fifth column gives the formal precision estimates of the coordinates in meters.

Station	X	Y	Z	σ	Station Name
1021	1.118029	-4.876316	3.942984	7	BLOSSOM POINT, MD.
1034	-.521702	-4.242049	4.718731	7	GRAND FORKS, MINN.
1042	.647515	-5.177924	3.656707	7	ROSMAN, N. C.
7036	-.828496	-5.657458	2.816812	7	EDINBURG, TEX.
7037	-.191286	-4.967280	3.983262	7	COLUMBIA, MO.
7039	2.308239	-4.873597	3.394580	10	BERMUDA
7040	2.465067	-5.534924	1.985510	10	PUERTO RICO
7045	-1.240479	-4.760229	4.048995	9	DENVER, COL.
7050	1.130674	-4.831368	3.994111	7	Goddard Space Flight Center
7075	.692628	-4.347059	4.600483	9	SUDBURY, ONT.
7076	1.384174	-5.905685	1.966533	10	JAMAICA
7815	4.578370	.457951	4.403134	5	HAUTE PROVENCE, FRANCE
7816	4.654337	1.959134	3.884366	5	STEPHANION, GREECE
7818	5.426329	-.229330	3.334608	15	COLOMB-BECHAR, ALGERIA
7901	-1.535757	-5.166996	3.401042	5	ORGAN PASS, N.M.
8015	4.578328	.457966	4.403179	5	HAUTE PROVENCE, FRANCE
8019	4.579466	.586599	4.386408	5	NICE, FRANCE
9001	-1.535757	-5.166996	3.401042	5	ORGAN PASS, N.M.
9002	5.056125	2.716511	-2.775784	7	PRETORIA, S.AFRICA
9003	-3.983776	3.743087	-3.275566	6	WOOMERA, AUSTRALIA
9004	5.105588	-.555228	3.769667	5	SAN FERNANDO, SPAIN
9005	-3.946693	3.366299	3.698832	10	TOKYO, JAPAN
9006	1.018203	5.471103	3.109623	9	NAINI TAL, INDIA
9007	1.942775	-5.804081	-1.796933	7	AREQUIPA, PERU
9008	3.376893	4.403976	3.136250	9	SHIRAZ, IRAN
9009	2.251829	-5.816919	1.327160	7	CURACAO, ANTILLES
9010	.976291	-5.601398	2.880240	5	JUPITER, FLA.
9011	2.280589	-4.914573	-3.355426	9	VILLA DOLORES, ARGENTINA
9012	-5.466053	-2.404282	2.242171	7	MAUI, HAWAII
9021	-1.936782	-5.077704	3.331916	15	MT. HOPKINS, ARIZ.
9023	-3.977766	3.725102	-3.303035	6	ISLAND LAGOON, AUSTRALIA
9025	-3.910437	3.376361	3.729217	10	DODAIRA, JAPAN
9028	4.903750	3.965201	.963872	12	ADDIS ABABA, ETHIOPIA
9029	5.186461	-3.653856	-.654325	12	NATAL, BRAZIL
9031	1.693803	-4.112328	-4.556649	15	COMODORO RIVADAVIA, ARGENTINA
9050	1.489753	-4.467478	4.287304	14	HARVARD, MASS.
9065	3.923411	.299882	5.002945	12	DELFT, HOLLAND
9066	4.331310	.567511	4.633093	7	ZIMMERWALD, SWITZERLAND
9074	3.183901	1.421448	5.322772	10	RIGA, LATVIA
9077	3.907421	1.602397	4.763890	10	UZGHOROD, U.S.S.R.
9080	3.920178	-.134738	5.012708	9	MALVERN, ENGLAND
9091	4.595157	2.039425	3.912650	5	DIOYSOS, GREECE
9113	-2.450011	-4.624421	3.635035	7	ROSAMUND, CAL.
9114	-1.264838	-3.466884	5.185467	12	COLD LAKE, CANADA
9115	3.121280	.592643	5.512701	17	Harestua, Norway
9117	-6.007402	-1.111859	1.825730	15	JOHNSTON ISL., PACIFIC

Table 14. Fully normalized coefficients of the spherical harmonic expansion of the geopotential obtained in the final iteration of the combination solution. $C_{\ell m}$ are the cosine terms of degree ℓ and order m and $S_{\ell m}$ are the sine terms.

ℓ	m	$C_{\ell m}$	$S_{\ell m}$	ℓ	m	$C_{\ell m}$	$S_{\ell m}$
2	2	2.4129E-06	-1.3641E-06	3	1	1.9698E-06	2.6015E-07
3	2	8.9204E-07	-6.3468E-07	3	3	6.8630E-07	1.4304E-06
4	1	-5.2989E-07	-4.8765E-07	4	2	3.3024E-07	7.0633E-07
4	3	9.8943E-07	-1.5467E-07	4	4	-7.9692E-08	3.3928E-07
5	1	-5.3816E-08	-9.7905E-08	5	2	6.1286E-07	-3.5087E-07
5	3	-4.3083E-07	-8.6663E-08	5	4	-2.6693E-07	8.3010E-08
5	5	1.2593E-07	-5.9910E-07	6	1	-9.8984E-08	3.7652E-08
6	2	5.4825E-08	-3.5175E-07	6	3	2.7873E-08	4.4626E-08
6	4	-4.0342E-10	-4.0388E-07	6	5	-2.1143E-07	-5.2264E-07
6	6	8.8693E-08	-7.4756E-08	7	1	2.4142E-07	1.1567E-07
7	2	2.8306E-07	1.5645E-07	7	3	2.0285E-07	-2.3448E-07
7	4	-1.9727E-07	-1.1390E-07	7	5	-8.7024E-10	9.8461E-08
7	6	-2.5847E-07	1.0209E-07	7	7	1.5916E-07	-6.7710E-08
8	1	3.1254E-08	2.5696E-08	8	2	4.8161E-08	8.4140E-08
8	3	-5.7444E-08	1.8086E-08	8	4	-1.5378E-07	7.5264E-08
8	5	-5.6733E-08	6.1636E-08	8	6	-5.3903E-08	2.5930E-07
8	7	3.4390E-08	8.9168E-08	8	8	-7.7364E-08	6.7607E-08
9	1	1.3823E-07	-1.6100E-08	9	2	6.6741E-09	-8.1733E-08
9	3	-9.6463E-08	-1.1817E-07	9	4	5.7125E-08	1.1183E-07
9	5	-6.1435E-09	3.3551E-09	9	6	2.4186E-08	2.2028E-07
9	7	-5.0450E-08	-1.2700E-07	9	8	2.3359E-07	5.7239E-08
9	9	-8.2490E-08	9.2326E-08	10	1	1.1251E-07	-1.0167E-07
10	2	-3.1225E-08	-1.0450E-07	10	3	-2.3346E-08	-1.4137E-07
10	4	-4.8185E-08	-4.3248E-08	10	5	-8.0004E-08	-1.4279E-07
10	6	-3.2486E-08	-2.0153E-07	10	7	5.4961E-08	3.2003E-08
10	8	7.3957E-08	-7.9706E-08	10	9	-6.8563E-09	6.2498E-09
10	10	1.2377E-07	-2.5885E-08	11	1	4.3900E-09	2.9751E-08
11	2	4.8900E-08	-9.1994E-08	11	3	-6.3247E-08	-1.3109E-07
11	4	-3.0193E-08	5.4317E-08	11	5	3.2523E-08	1.3215E-07
11	6	3.7517E-08	6.9005E-09	11	7	4.5726E-08	-1.3862E-07
11	8	6.4546E-08	-1.6993E-08	11	9	1.1750E-07	-9.9451E-09
11	10	-1.1736E-07	-1.8900E-08	11	11	1.1785E-07	-4.0688E-08
12	1	-4.5955E-08	-3.1000E-08	12	2	2.7481E-08	7.5986E-08
12	3	5.8386E-08	5.4784E-08	12	4	-4.3649E-08	-2.2262E-08
12	5	2.3375E-08	4.2637E-08	12	6	-2.3868E-08	-6.6770E-10
12	7	1.4507E-08	9.9784E-08	12	8	-5.7854E-09	3.3752E-08
12	9	-3.2232E-08	4.2859E-08	12	10	-1.8590E-08	4.8382E-09
12	11	-4.4921E-08	-4.8206E-08	12	12	-1.9407E-08	-5.7771E-08
13	1	-5.6042E-08	2.6288E-08	13	2	-4.7456E-08	1.7367E-08
13	3	2.3833E-08	-2.8930E-08	13	4	-1.9980E-08	5.7030E-08
13	5	9.6637E-08	-4.7760E-08	13	6	-8.3417E-08	5.9782E-08
13	7	-5.2217E-08	-3.2562E-09	13	8	-4.1759E-08	-2.0231E-08
13	9	-2.5623E-08	1.0767E-07	13	10	8.6589E-08	-1.0528E-08
13	11	-3.3749E-08	5.8541E-08	13	12	-1.3229E-09	8.2192E-08
13	13	-7.0288E-08	7.4643E-08	14	1	-2.3090E-08	4.9664E-08
14	2	3.2120E-08	-4.5289E-08	14	3	1.9042E-08	1.1919E-09
14	4	7.8017E-09	-3.7527E-08	14	5	-2.5958E-08	-2.3344E-08
14	6	1.9140E-08	-5.8721E-08	14	7	1.1061E-08	8.4132E-09
14	8	-3.0273E-08	-6.0838E-08	14	9	4.9539E-08	9.2345E-08
14	10	5.3732E-08	-4.3168E-08	14	11	2.7833E-08	-8.1637E-08
14	12	1.2481E-08	-5.7314E-08	14	13	5.1554E-08	4.5453E-08
14	14	-5.2082E-08	-1.2840E-08	15	1	-3.5971E-09	4.0142E-08
15	2	-4.4833E-08	-1.6056E-08	15	3	8.3016E-09	-5.7218E-09
15	4	1.3916E-08	6.6644E-08	15	5	3.1684E-08	1.8250E-09
15	6	7.0020E-08	-1.1872E-07	15	7	1.1856E-07	4.2690E-08
15	8	-9.7657E-08	-3.5710E-08	15	9	2.2064E-08	2.6632E-08
15	10	-2.0648E-08	5.3724E-10	15	11	-3.2585E-08	9.4052E-08
15	12	1.0524E-08	6.8726E-09	15	13	-3.7348E-08	4.0249E-09
15	14	1.2193E-08	-2.6786E-08	15	15	1.4515E-09	-1.4802E-08
16	1	-2.3789E-08	7.6413E-08	16	2	2.1327E-08	3.0669E-08
16	3	-4.7358E-08	3.2610E-08	16	4	-1.1591E-08	4.3001E-08
16	5	-4.4201E-08	3.2230E-08	16	6	-5.8439E-08	-4.2809E-08
16	7	1.0591E-07	8.1008E-09	16	8	-8.4738E-08	-2.4677E-09
16	9	9.0001E-09	-1.0628E-07	16	10	-2.9849E-08	-5.2467E-10
16	11	6.8502E-09	-7.0765E-08	16	12	2.2834E-08	-3.4087E-08
16	13	3.5475E-08	2.0683E-08	16	14	-7.3590E-09	-2.2626E-08
16	15	-3.5485E-08	8.4126E-10	16	16	-2.9522E-08	8.6217E-09
17	12	8.3097E-08	3.5424E-09	17	13	3.2749E-08	4.2920E-10
17	14	-1.6058E-08	2.7286E-08	18	12	1.1662E-08	8.4724E-09
18	13	4.6903E-09	-3.5547E-08	18	14	-2.7446E-08	-4.8376E-08
19	12	6.7115E-08	-8.2623E-09	19	13	3.3201E-08	-6.3128E-08
19	14	-3.9779E-09	-2.3817E-08	20	13	5.8374E-08	3.3320E-08
20	14	1.1130E-08	-1.6183E-08	21	13	3.6928E-09	-1.6288E-08
21	14	5.2067E-08	3.0801E-10	22	14	-8.0549E-09	2.6440E-08

The degree variances $\sigma_\ell^2 = 1/(2\ell+1) \sum_{m=0}^{\ell} (C_{\ell m}^2 + S_{\ell m}^2)$ of the combination solution are given in Figure 5 for $\ell \geq 6$. They show a remarkable adherence to the rule of thumb $\sigma_\ell = 10^{-5}/\ell^2$.

Figure 6 gives the geoid corresponding to the new combination solution and a flattening of 1/298.255, Figure 7 the geoid corresponding to the hydrostatic flattening of 1/299.67, and Figure 8 a plot of the free-air gravity anomalies corresponding to the combination solution.

Table 13 contains the accuracy estimates of the station coordinates. These estimates are the formal statistics from the combination solution, but as the subsequent comparisons show, they appear to be realistic.

Figure 9 illustrates the precision estimates of the geoid heights as computed from the precision estimates of the spherical harmonic coefficients. In this computation the correlation between coefficients has been ignored because the correlation coefficients are generally less than 0.2. This neglect, and the fact that for equal degree and order $\sigma_{C_{\ell m}}^2 \approx \sigma_{S_{\ell m}}^2$, means that the geoid-height precision estimates are essentially longitude independent and symmetric about the equatorial plane. Kozai's accuracy estimates for his zonal harmonics were included in this calculation. Subsequent comparisons with surface gravity and astrogeodetic data show that these precision estimates are quite realistic, and the geoid appears to be determined with an accuracy of 3 to 4 m. Of course, these accuracy estimates refer to the generalized geoid and do not imply that the geoid is everywhere known with this accuracy. In areas such as the South Pacific where there are no surface-gravity data and where the gravity field cannot be directly sampled, the uncertainty in geoid height may be larger than the 3 or 4 m.

Comparison of Geometric and Dynamic Satellite Solutions

Figure 10 and Table 15 show the results for the comparisons of the directions computed by the two solutions. The accuracy estimates given by the two solutions are indicated by the error ellipses. The difference δ in the positions derived from the individual solutions is a good indication of the accuracies that may be expected for the combination-solution coordinates, though it must

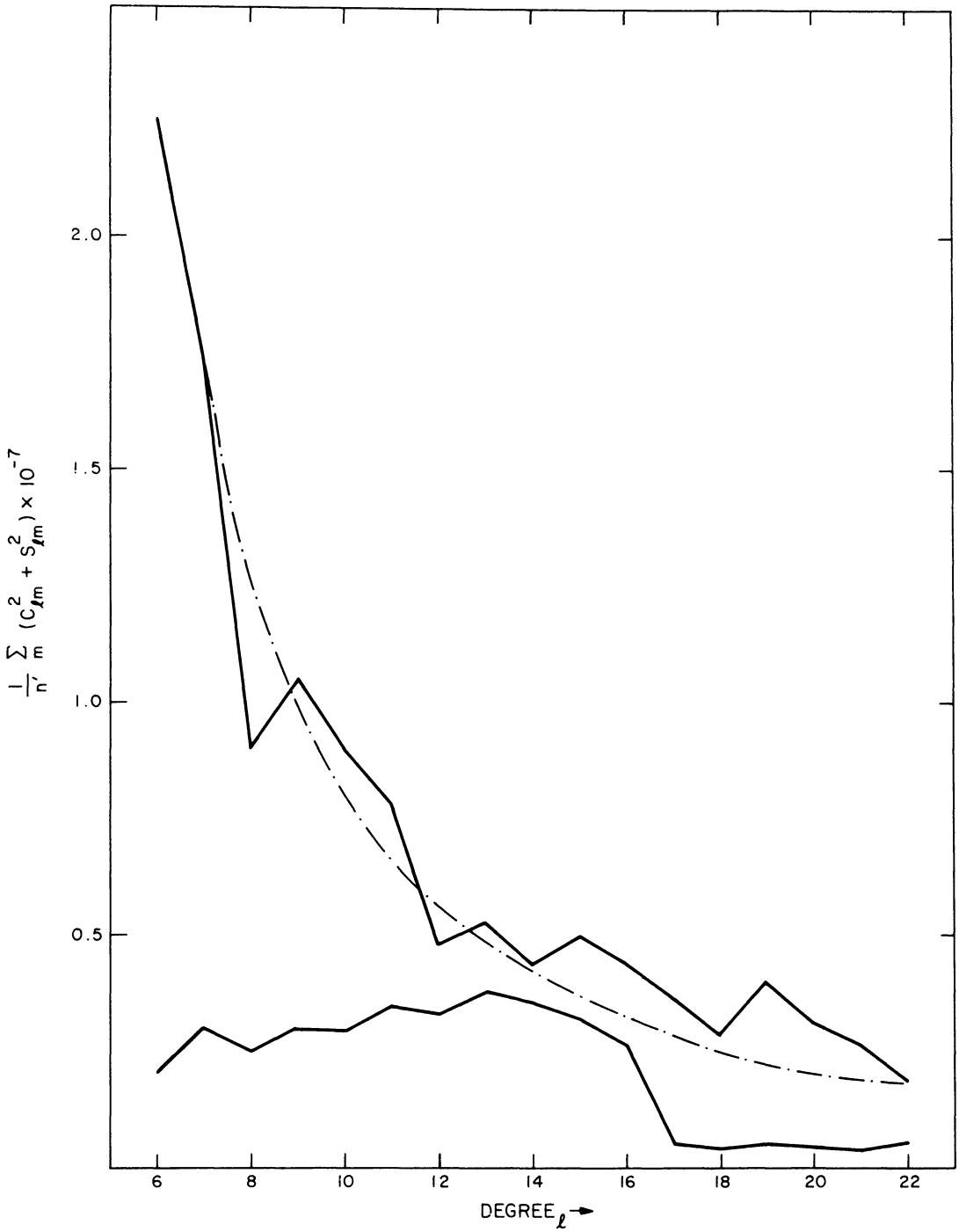

Fig. 5. Degree variances for $6 < \ell < 22$ for the combination solution. Kaula's rule of thumb is indicated by the dashed line. For $2 < \ell < 6$ the degree variances are in complete agreement with this rule. The lower curve gives the degree variances corresponding to the precision estimates of the harmonics, i.e., $1/n' \sum_m \left(\sigma^2_{C_{\ell m}} + \sigma^2_{S_{\ell m}}\right)$.

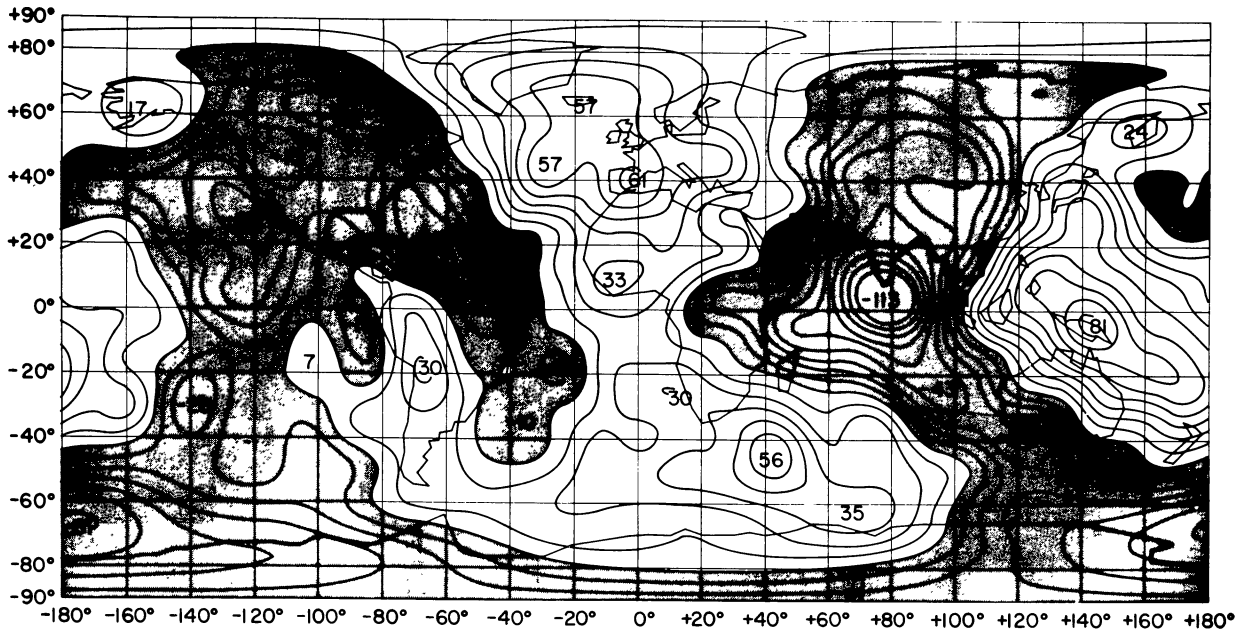

Fig. 6. Geoid heights in meters of the new combination solution corresponding to a reference ellipsoid of flattening f = 1/298.255.

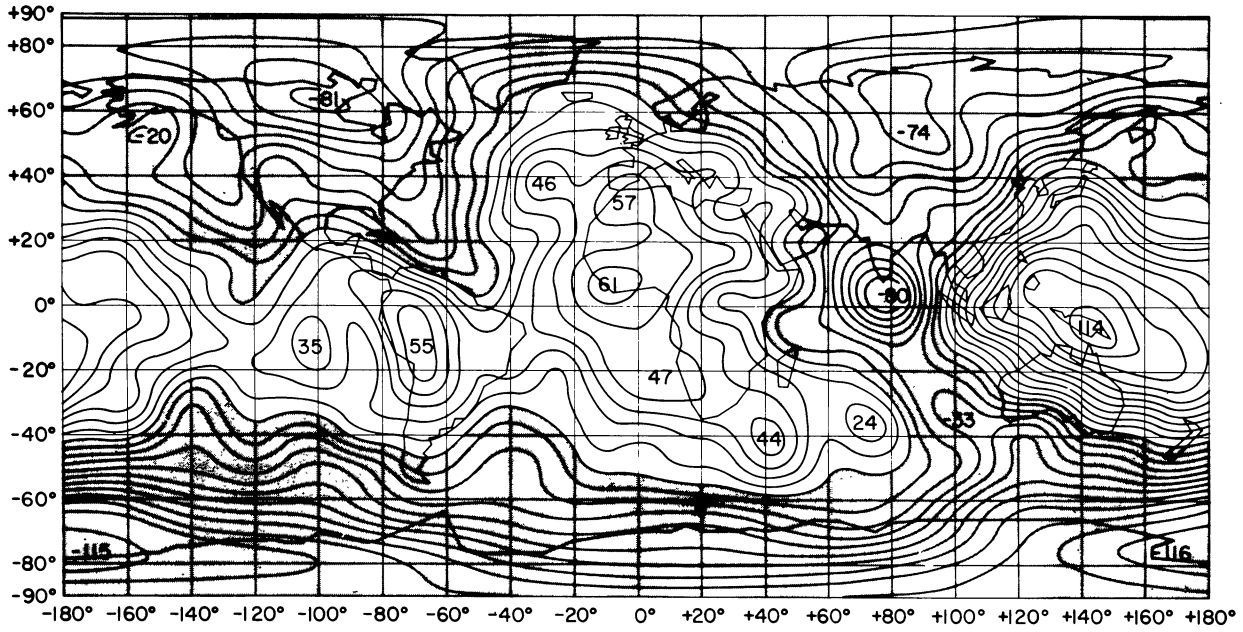

Fig. 7. Geoid heights in meters of the new combination solution corresponding to a reference ellipsoid of flattening f = 1/299.67.

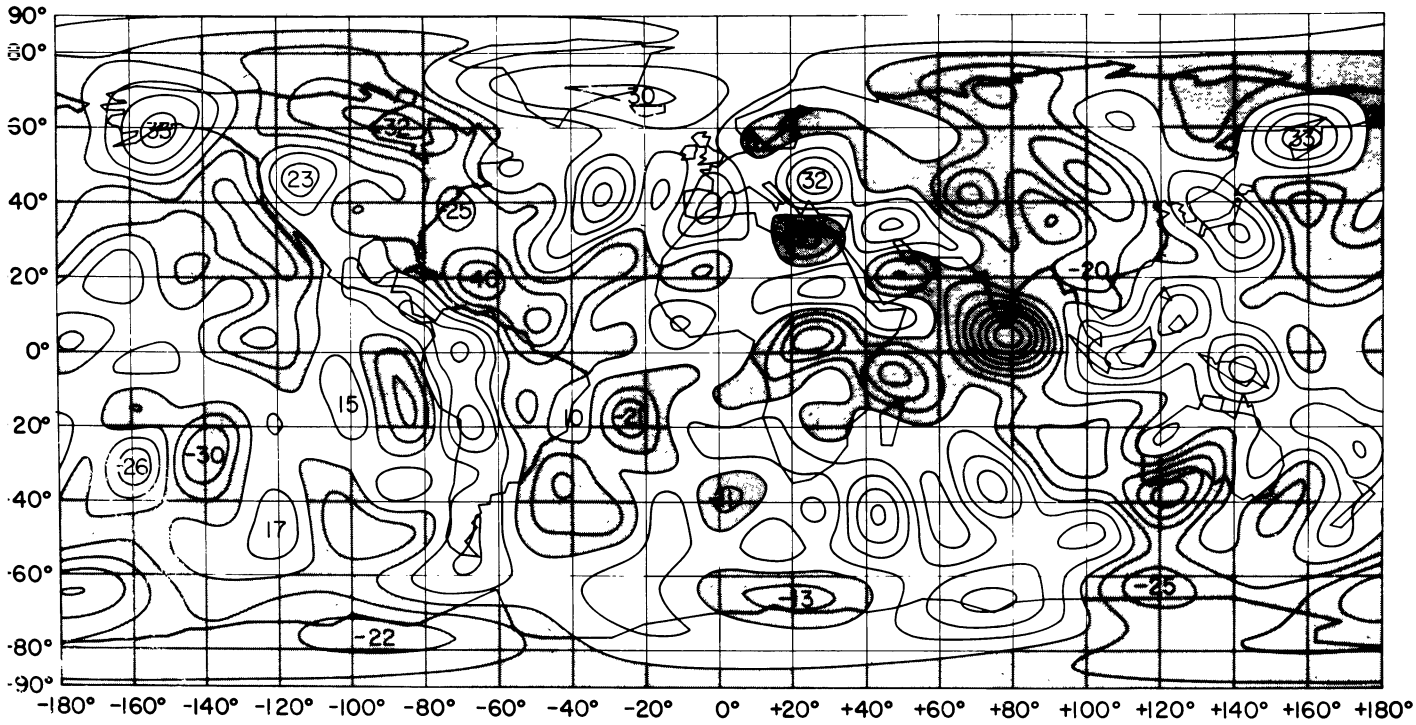

Fig. 8. Gravity anomalies with respect to the best fitting ellipsoid f = 1/298.255 from the adopted solution (10-mgal contours).

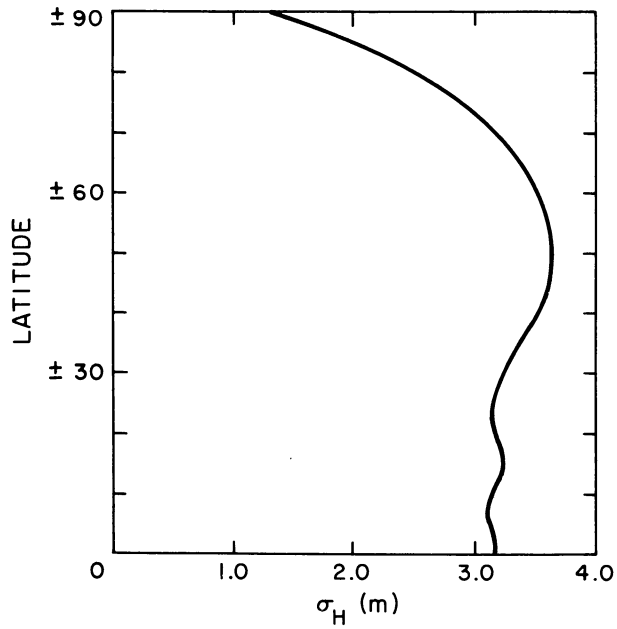

Fig. 9. Precision estimates of geoid heights determined from the harmonic coefficient precision estimates.

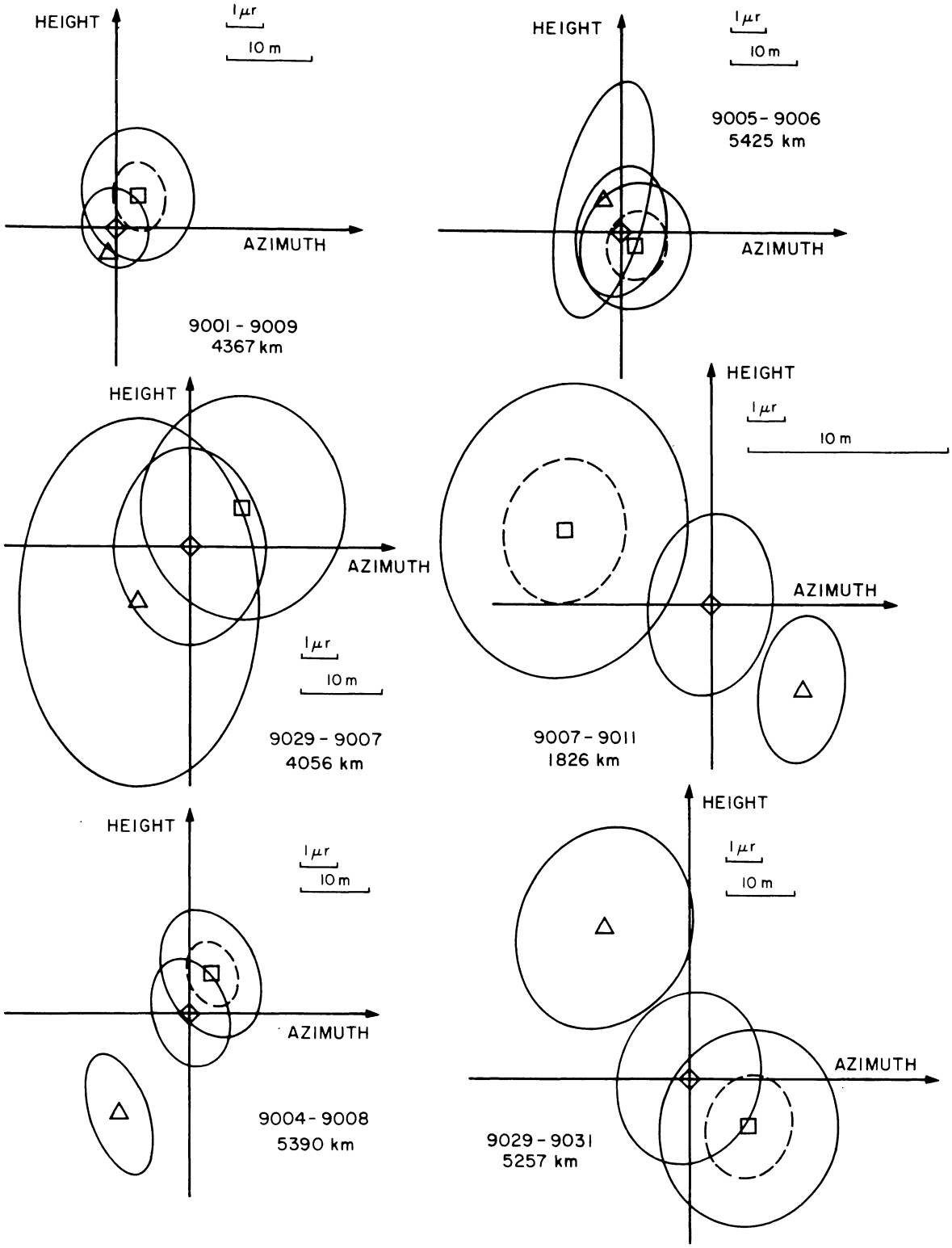

Fig. 10. Comparisons for station-station vectors computed from the geometric solution △, the dynamic solution □, and the combination solution ◇. The two error ellipses centered at □ refer to the formal statistics of the dynamic solution (the inner ellipse) and after the covariance matrix has been multiplied by the factor k_1^2 (outer ellipse).

be pointed out that in Figure 10 the difference between the two solutions results from uncertainties in the coordinates of both stations, and that at each station a number of such comparisons can usually be made. Thus, the accuracy of the station positions relative to the origin of the coordinate system should be better than these figures indicate.

TABLE 15. Summary of differences δ between directions computed from the geometric solution with accuracy σ_G and from the dynamic solution with accuracy σ_D (μrad). k is the factor by which the latter estimates must be scaled.

Line	σ_G^2	σ_D^2	δ^2	k^2
9001–9009	2.6	0.7	3.2	1.8
9001–9010	2.8	0.9	7.8	4.1
9001–9012	6.5	0.2	3.2	0.9
9002–9028	39.0	1.3	57.8	2.9
9004–9008	4.7	0.7	20.2	7.5
9004–9009	14.1	0.4	25.0	3.3
9004–9010	15.1	0.2	10.9	1.4
9004–9028	9.4	0.8	16.0	3.1
9004–9029	28.9	1.0	51.9	3.5
9005–9006	16.1	0.8	2.6	0.3
9005–9012	61.1	0.6	15.2	0.4
9006–9008	13.5	2.2	6.3	0.8
9007–9009	3.9	1.8	39.6	13.6
9007–9010	2.6	0.5	30.2	18.9
9007–9011	6.8	3.6	60.9	11.7
9007–9029	16.4	2.3	14.4	1.5
9007–9031	17.7	2.1	20.1	2.0
9009–9010	6.5	3.7	18.4	3.6
9009–9011	2.3	0.8	13.0	8.1
9028–9091	23.9	1.5	96.0	7.6
9029–9031	17.7	1.6	44.9	4.6
				$k_{AV}^2 = 4.9$

The accuracy estimates σ_G of the geometric solution directions are obtained by the method described in Section 4. The dynamic solution, however, gives accuracy estimates for the coordinates — and consequently for the station-station vectors σ_D — that are overoptimistic. This is usually evident from figures such as Figure 10 where δ^2 is often considerably greater than either σ_D^2 or σ_G^2. Making an analysis similar to that used in the geometric solution for establishing the accuracy indicates that the covariance matrix of the dynamic solution should be multiplied by a factor of $k_1^2 = 4.5$. When harmonic coefficients derived from different iterations of the dynamic satellite solution are compared, it also appears that the formal variances must be multiplied by a factor of about 5 in order to obtain realistic accuracy estimates.

Figure 10 also indicates the directions of the station-station vector derived from the combination solution compared with the geometric and dynamic results. In view of the above comment about the interpretation of these comparisons, they indicate that for the fundamental Baker-Nunn stations (those numbered 9001 to 9012) the combination-solution coordinates should be reliable to better than 10 m. For the new Baker-Nunn stations (9021, 9028, 9029, 9031, and 9091), from which there are fewer observations, the comparisons indicate that the combination-solution coordinates should be reliable to better than 15 m. These estimates are in agreement with the formal statistics given in Table 13. The longitude difference between the two satellite solutions obtained from the combination solution is -0.2 ± 0.5 μrad and is not significant.

Comparison with Satellite Orbits

Each solution resulted in improved orbital residuals; for the final solution the orbital residuals for satellites such as Geos 1 or Geos 2 are less than 10 m. These orbits are computed from a combination of laser and Baker-Nunn data for 30 days. The residuals for the optical data are less than 2 arcsec. The laser data have an accuracy of 1 to 2 m. The rms is 7 m in all cases and no residuals exceed 10 m. These are orbits with significant

amounts of laser data from 2 or 3 stations. The 7-m orbital errors can arise from station-coordinate errors (probably about 5 m), geopotential errors (possibly 5 m), and unmodeled periodic perturbations.

Comparison of Satellite and Deep-Space-Probe Solutions

In order to compare the satellite and JPL solutions, a combination solution using only the satellite and surface-gravity information has been made. Table 16 indicates the results for those Baker-Nunn stations that are related to the JPL antennas. From the ground-survey information given in Table 10, the coordinates for the JPL sites in the SAO system can be computed and the differences in longitude $\Delta\lambda_i$ and in distance to the rotation axis Δr_i are given in Table 17. This table also gives the accuracy estimates from the statistics provided by the two solutions and ground survey. The differences in longitude immediately reflect the systematic longitude differences between the two solutions: the JPL longitudes are to the east of the SAO longitudes. From the overall combination solution discussed in Section 7, these transformation parameters are solved for and yield $\overline{\Delta\lambda} = -3.2 \pm 0.5$ μrad and $\frac{\Delta r}{r} = (+0.3 \pm 0.5)\,10^{-6}$, the scale of the SAO system as defined by the station coordinates being larger than that of the JPL system.

TABLE 16. Coordinates for Baker-Nunn stations derived from a combination of the geometric and dynamic satellite solutions and surface gravity only.

Station	X (Mm)	Y (Mm)
9002	5.056126	2.716511
9003	-3.983778	3.743085
9004	5.105587	-0.555230
9113	-2.350466	-4.651977

TABLE 17. Results of SAO-JPL stations comparison. $\Delta\lambda_i$ is the longitude difference and Δr_i the difference in distance to the earth's axis of rotation for the two solutions. $\overline{\Delta\lambda}$ is the weight mean longitude difference.

Stations	$\lambda_{SAO}-\lambda_{JPL}=\Delta\lambda_i$ (μrad)	$\overline{\Delta\lambda}-\Delta\lambda_i$ (μrad)	$\overline{\Delta\lambda}-\Delta\lambda_i$ (m)	$\sigma_{\Delta\lambda_i}$ (m)^i	$r_{SAO}-r_{JPL}=\Delta r_i$ (m)	$\sigma_{\Delta r_i}$ (m)^i
4751-9002	-3.5	+0.3	+1.9	7.7	+5.9	4.9
4741-9003	-2.2	-0.9	-5.2	6.8	-7.3	4.5
4742-9003	-1.2	-2.0	-10.4	9.0	-6.5	4.5
4761-9004	-4.5	+1.4	+6.9	6.6	-1.2	4.5
4712-9113	-4.9	+1.7	+9.2	12.4	+7.6	5.5

The residuals $\overline{\Delta\lambda}-\Delta\lambda_i$ and $\overline{\Delta r}-\Delta r_i$ are in all cases less than 10 m and support the accuracy estimates given in Table 13 for stations 9002, 9003, 9004, and 9113. Table 18 gives the adjusted coordinates of the JPL stations in the SAO reference system.

TABLE 18. Coordinates of the JPL stations referred to the SAO reference system.

Station	X (Mm)	Y (Mm)	Z (Mm)
4751	5.085451	2.668252	-2.768728
4741	-3.978706	3.724858	-3.302213
4742	-4.460972	2.682424	-3.674618
4761	4.849242	-0.360290	4.114869
4712	-2.350454	-4.651975	3.665631

The longitude difference cannot be attributed to the difference in the UT1 time systems used by the two agencies, since at the time of the Mariner 5 observations UT1(JPL) - UTC = 89.0 msec and UT1(SAO) - UTC = 101.4 msec, so that the expected longitude difference would be +12 msec or 0.8 μrad.

The total unexplained longitude difference is, therefore, -4.0 μrad. This discrepancy appears to be due to different definitions of the right ascension of the vernal equinox. In the case of SAO this is defined by the star positions given in the SAO catalog — which refers to the FK4 system — and in the case of JPL the vernal equinox is defined in the planetary ephemeris used [Melbourne and O'Handley, 1968].

The scale difference between the two solutions is hardly significant in view of the standard deviation. This would be expected since both solutions have used the same GM value.

Comparison with Surface Gravity

To compare the satellite solution with the surface gravity, the following quantities defined by Kaula [1966a] have been computed:

$\langle g_T^2 \rangle$ mean value of g_T^2, where g_T is the mean free-air gravity anomaly based on surface gravity, indicating the amount of information contained in the surface-gravity anomalies;

$\langle g_S^2 \rangle$ mean value of g_S^2, where g_S is the gravity anomaly derived from the satellite solution, indicating the amount of information contained in the satellite-gravity anomalies;

$\langle g_T g_S \rangle$ an estimate of the mean square of g_H, the true value of the contribution to the gravity anomaly of the estimates of geopotential coefficients from the satellite solution, the amount of information common to the surface-gravity and satellite-gravity anomalies;

$\langle (g_T - g_S)^2 \rangle$ mean square difference of the g_S and g_T;

$E\{\epsilon_S^2\}$ mean square of the satellite error;

$E\{\epsilon_T^2\}$ mean square of the surface-gravity error;

$E\{\delta g^2\}$ mean square of the error of omission, the difference between the true gravity anomaly and g_H.

If the satellite solution gave a "perfect" estimate of the $C_{\ell m}$ and $S_{\ell m}$, that is, $\langle g_S^2 \rangle = \langle g_H^2 \rangle$ $(\equiv \langle g_T g_S \rangle)$, then ϵ_S^2 would be zero even through g_S would not contain all the information necessary to describe the total field. The information not contained in the satellite field — the error of omission δg — then consists of the neglected higher order coefficients. The quantity $\langle (g_T - g_S)^2 \rangle$ provides a measure of the agreement between the two estimates, g_T and g_S, of the gravity field and is equal to the sum of the estimates of the three types of errors. Thus,

$$(g_T - g_S)^2 = E\{\epsilon_S^2\} + E\{\epsilon_T^2\} + E\{\delta g^2\} \quad .$$

Another estimate of g_H can be obtained from the gravimetric estimates of degree variances σ_ℓ^2 [Kaula, 1966a],

$$E\{g_H^2\} = D = \sum_\ell \frac{n_\ell}{2\ell+1} \sigma_\ell^2 \quad ,$$

where n_ℓ is the number of coefficients of degree ℓ included in g_H. Table 19 gives the σ_ℓ^2 for degree 0 to 16 as well as the degree variances of the satellite and combination solution computed from

$$\sigma_\ell^2 = \gamma^2 (\ell - 1)^2 \sum_m \left(C_{\ell m}^2 + S_{\ell m}^2 \right) \quad .$$

If both the satellite solution and the surface gravity gave "perfect" results for terms up to a given degree, then

$$\langle g_S^2 \rangle = \langle g_T g_S \rangle = D \quad \text{and} \quad E\{\boldsymbol{\varepsilon}_S^2\} = E\{\boldsymbol{\varepsilon}_T^2\} = 0 \quad .$$

TABLE 19. Power spectra of free-air gravity anomalies.

Degree	Degree Variance ($mgal^2$)		
	Gravimetric Solution	Satellite Solution	Combination Solution
0	2.9		
1	-0.2		
2	5.9	7.4	7.4
3	31.0	33.3	33.0
4	18.2	19.7	20.0
5	7.3	17.5	17.8
6	20.7	14.4	15.7
7	9.2	16.4	15.5
8	7.0	8.5	6.7
9	8.7	15.1	12.7
10	9.4	17.7	12.9
11	5.7	13.7	12.2
12	3.5	8.4	5.1
13	7.0		11.1
14	9.4		8.4
15	9.9		13.2
16	5.5		13.8

Table 20 summarizes the estimates obtained for these quantities from the satellite solution, the combination solution, and the Gaposchkin [1966] M1 solution. All three sets contain the same zonal harmonics. The estimates are given for three sets of 300-n mi squares: (1) the squares for which the number n of observed 60-n mi squares is equal or greater than 1, (2) the squares for which $n \geq 10$, and (3) the squares for which $n \geq 20$. For the last data set the comparisons are made for the three fields truncated for different degree as well as for the total fields.

The variations between the estimates obtained for the three types of errors, $E\{\epsilon_S^2\}$, $E\{\epsilon_T^2\}$, and $E\{\delta g^2\}$, result from the assumptions made about the complete randomness of the quantities g_H, δg, ϵ_T, and ϵ_S.

TABLE 20. Comparison of satellite and combination solutions with surface-gravity measurements ($mgal^2$).

Solution	$\langle(g_T-g_S)^2\rangle$	$\langle g_T g_S\rangle$	$\langle g_S^2\rangle$	D	$\langle g_T^2\rangle$	$E\{\epsilon_S^2\}$	$E\{\epsilon_T^2\}$	$E\{\delta g^2\}$
		$n \geq 1$, N = 935, 300-n mi squares						
Combination Solution	206	146	225	163	274	79	72	56
Satellite Solution	272	110	218	143	274	108	72	92
M1 Solution	242	90	148	108	274	58	72	79
		$n \geq 10$, N = 369, 300-n mi squares						
Combination Solution	135	195	230	163	297	35	19	83
Satellite Solution	250	127	212	143	297	85	19	151
M1 Solution	222	102	131	108	297	29	19	176
		$n \geq 20$, N = 136, 300-n mi squares						
Combination Solution								
$\ell \leq 8$ $m \leq 8$	165	90	92	102	253	2	11	152
$\ell \leq 10$ $m \leq 10$	132	119	116	120	253	-3	11	123
$\ell \leq 11$ $m \leq 11$	135	126	134	126	253	8	11	116
$\ell \leq 12$ $m \leq 12$	134	129	138	129	253	9	11	113
$\ell \leq 14$ $m \leq 14$	109	156	166	146	253	10	11	87
$\ell \leq 16$ $m \leq 16$	75	184	186	163	253	2	11	58
		$n \geq 20$, N = 136, 300-n mi squares						
Satellite Solution								
$\ell \leq 8$ $m \leq 8$	179	86	98	102	253	12	11	156
$\ell \leq 10$ $m \leq 10$	145	109	110	120	253	1	11	133
$\ell \leq 11$ $m \leq 11$	151	115	126	126	253	11	11	127
$\ell \leq 12$ $m \leq 12$	163	111	128	129	253	17	11	131
$\ell \leq 14$ $m \leq 14$	173	117	150	146	253	33	11	125
Total Field	177	118	161	143	253	43	11	124
		$n \geq 20$, N = 136, 300-n mi squares						
M1 Solution								
$\ell \leq 8$ $m \leq 8$	168	85	85	102	253	0	11	157
Total Field	168	93	101	108	253	7	11	148

The combination solution gives the best results in that there is good agreement between the three estimates $\langle g_S^2\rangle$, $\langle g_T g_S\rangle$, and D of $\langle g_H^2\rangle$ and the $E\{\epsilon_S^2\}$ and $\langle(g_S-g_T)^2\rangle$ are small. The negative value for $E\{\epsilon_S^2\}$ when $\ell = 10$ is caused by the combination solution containing the gravity anomalies against which the tests are made. The estimates of the errors of omission are still quite large when compared with the estimates of ϵ_S^2 and ϵ_T^2, indicating that the surface-gravity data have additional information that has not been extracted in this solution.

The results obtained from the satellite solution alone are not in so good agreement with the surface-gravity data as the combination solution. For a gravity field complete to 8, 8, the M1 and the new satellite solution give

almost equivalent comparisons. For both, the $E\{\epsilon_S^2\}$ are small and there is good agreement between $\langle g_T g_S \rangle$, $\langle g_S^2 \rangle$, and D, indicating that the two solutions are equivalent and that they contain most of the information in a "correct" 8, 8 field. At 10, 10 the new satellite solution shows a marked improvement in the comparison $\langle (g_T - g_S)^2 \rangle$, and this field also appears to be as good as may be expected. But beyond about the 11th order the comparisons deteriorate and the $E\{\epsilon_S^2\}$ increase.

Further tests with surface-gravity data were made by use of the recent compilations by Talwani and Le Pichon [1969] for the Atlantic Ocean and for the Indian Ocean [Le Pichon and Talwani, 1969]. Figure 11 shows free-air gravity-anomaly profiles computed from 5° × 5° area means from these compilations and from the combination solution. With the exception of the first, these profiles are taken along the ships' tracks where continuous gravity measurements were obtained. The first profile, along latitude 32.°5 in the North Atlantic, is midway between two parallel ship cruises. All profiles are referenced to the international gravity formula. The accuracy of the 5° × 5° area means is assumed to be 5 mgal.

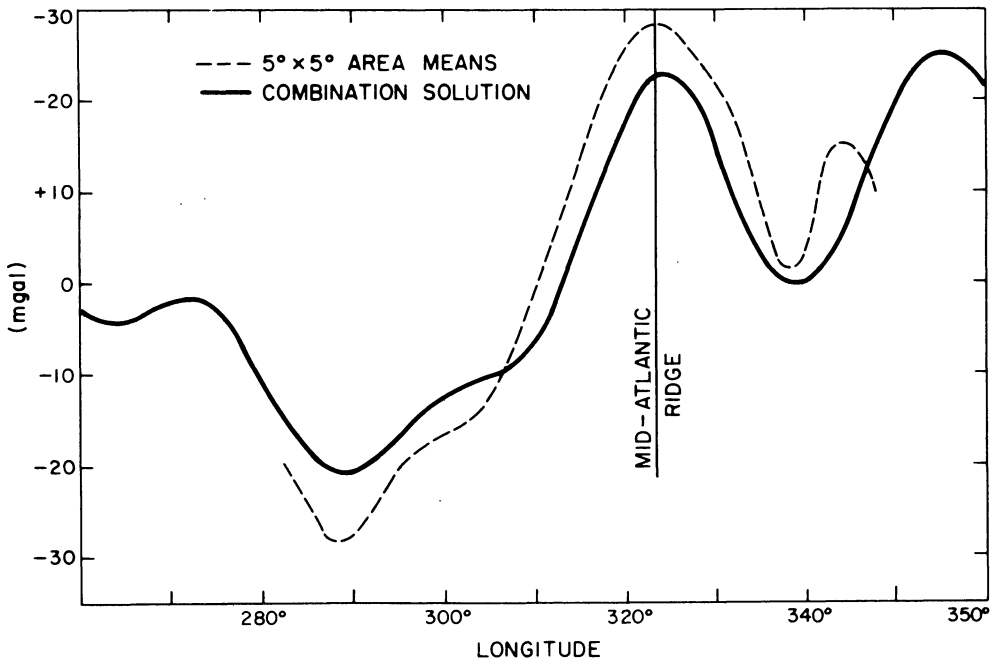

North Atlantic
$\Phi = +32.^{\circ}5$

Fig. 11. Comparisons of continuous gravity profiles from shipboard measurements compiled by Talwani and Le Pichon (broken lines) with profiles computed from the combination solution (solid lines).

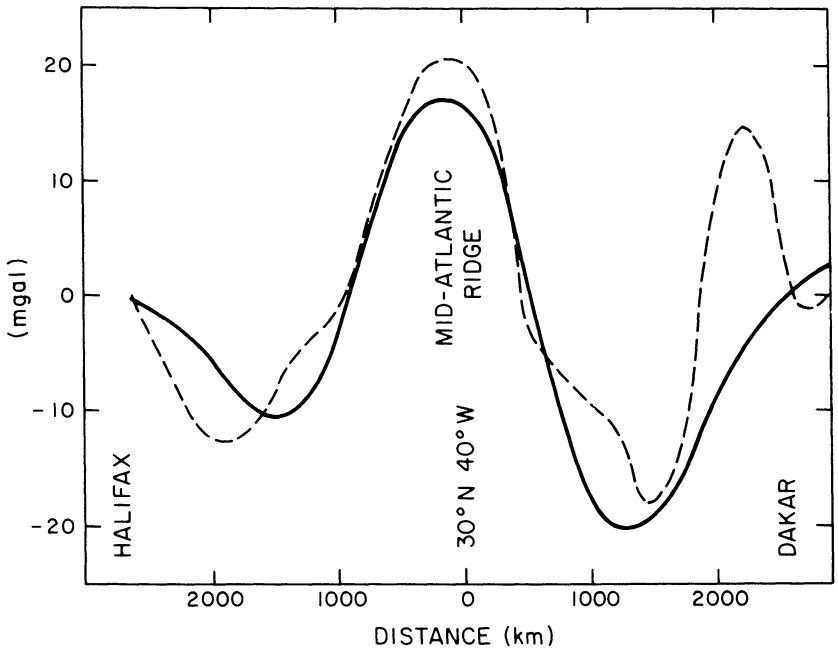

North Atlantic
Northwest–Southeast
Profile from Halifax to Dakar

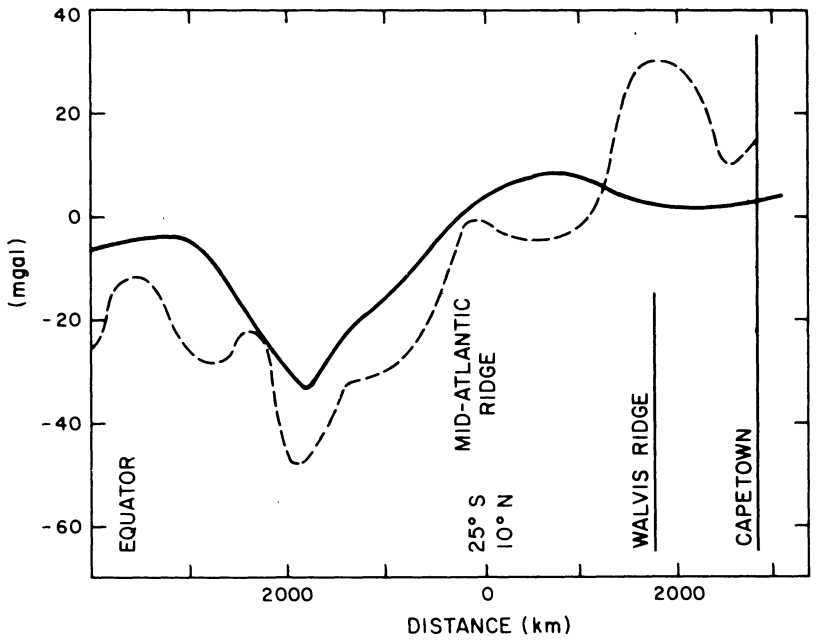

South Atlantic
Northwest–Southeast
Profile from Equator to Capetown

Fig. 11 (Cont.)

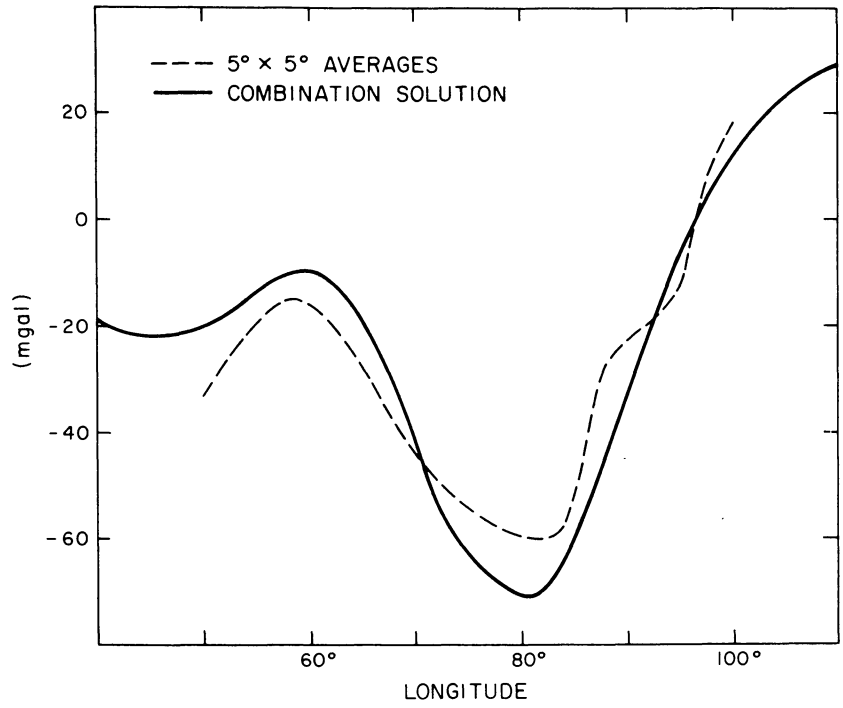

Indian Ocean
$\Phi = 0°$

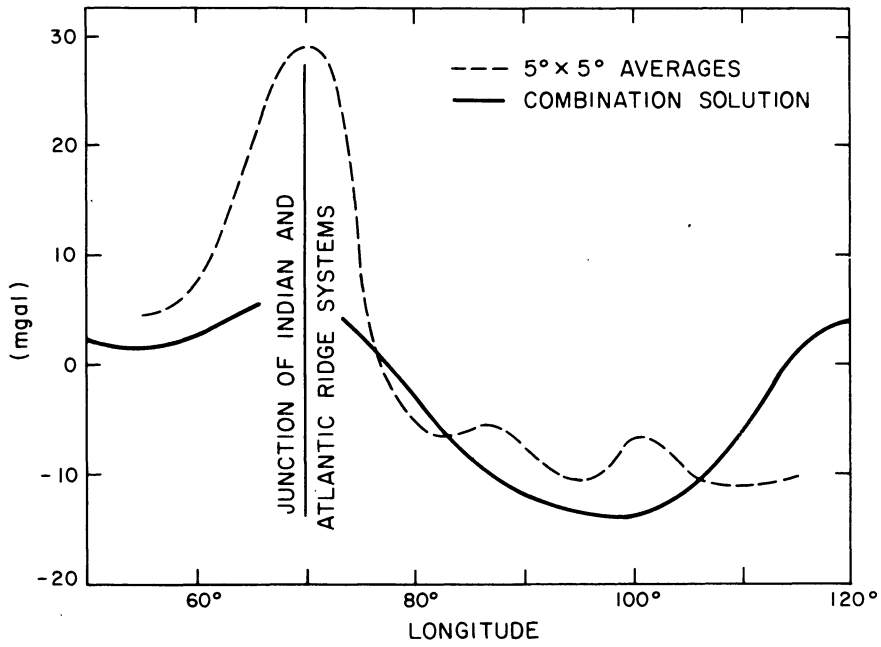

Indian Ocean
$\Phi = -25°$

Fig. 11 (Cont.)

Table 21 gives $\langle (g_S - g_T)^2 \rangle$ for each of these profiles, and from these numbers the accuracy of the gravity anomalies computed from the combination solution can be computed. The average value is 10 mgal or about 3.5 m in geoid height. This average accuracy estimate is in good agreement with the previous estimates.

TABLE 21. Summary of comparisons between surface-gravity measurements g_T by Talwani and Le Pichon and gravity anomalies g_S computed from the combination solution for selected profiles.

Profile	$\langle (g_S - g_T)^2 \rangle$ (mgal^2)	$\sigma^2_{g_T}$ (mgal^2)	$\sigma^2_{g_S} = \langle (g_S - g_T)^2 \rangle - \sigma^2_{g_T}$ (mgal^2)
$\phi = 32.^\circ 5$ North Atlantic	84	25	59
NW-SE North Atlantic	68	25	43
NW-SE South Atlantic	222	25	197
$\phi = 0^\circ$ Indian Ocean	80	25	55
$\phi = -25^\circ$ Indian Ocean	166	25	144
			$(\sigma^2_{g_S})_{AV} = 99$ mgal$^2 \approx 10$ m^2

Comparison with Astrogeodetic Data

Geoid heights obtained from astrogeodetic leveling are available for several major datums. These data, like the surface-gravity data, could be used as a further input in the combination solution. However, the coverage extends only to areas where reliable surface-gravity data are also available, and the contribution of the additional information to the global solution is not very significant. Instead, the astrogeodetic data have been used for comparison purposes, thus providing an independent estimate of the accuracy of the global solution.

To compare astrogeodetic geoid profiles with the global solution it is necessary that the former refer to an ellipsoid, centered at the earth's mass center and of the same dimensions and parallel to the ellipsoid of reference

used for the global solution. The transformation elements are given for several major datums by Lambeck [1970]. When these transformations contain rotation elements, at least part of the systematic errors in the astrogeodetic heights is absorbed. In the case of the Indian Datum only one station is available for establishing the relationship between the datum and the global solution. Thus only the three translation elements could be determined and a systematic tilt may be expected.

The following comparisons were made:

1. the geoid section along the 34th parallel in North America given by Rice [1962];

2. a section along the meridian of 260° from 65° North to 18° North, selected from the compilation by Fischer, Slutsky, Shirley, and Wyatt [1967] for the North American Datum (NAD);

3. two profiles across Australia, one along the latitude circle of -30° and the other along the meridian of 138°, given by Fischer and Slutsky [1969];

4. a profile along the meridian of 75° through India [Survey of India, 1957];

5. a profile along the meridian of 16° through central Europe [Fischer, 1967].

Figure 12 gives the results. All profiles refer to a reference ellipsoid with a = 6378155 m and 1/f = 298.25. The astrogeodetic profiles are smoothed to remove any information with a half-wavelength of less than about 200 km.

The accuracy of the astrogeodetic profiles was assumed to be of the order of 1.5 m. This is somewhat greater than the accuracy generally stated for this type of observation (e.g., Bomford [1962]), but the stochastic nature of the transformation elements also has to be considered.

Table 22 summarizes the results of the comparisons. The average value of σ_S is 3.2 m and is in agreement with the earlier derived accuracy estimates for the geoid heights of the combination solution.

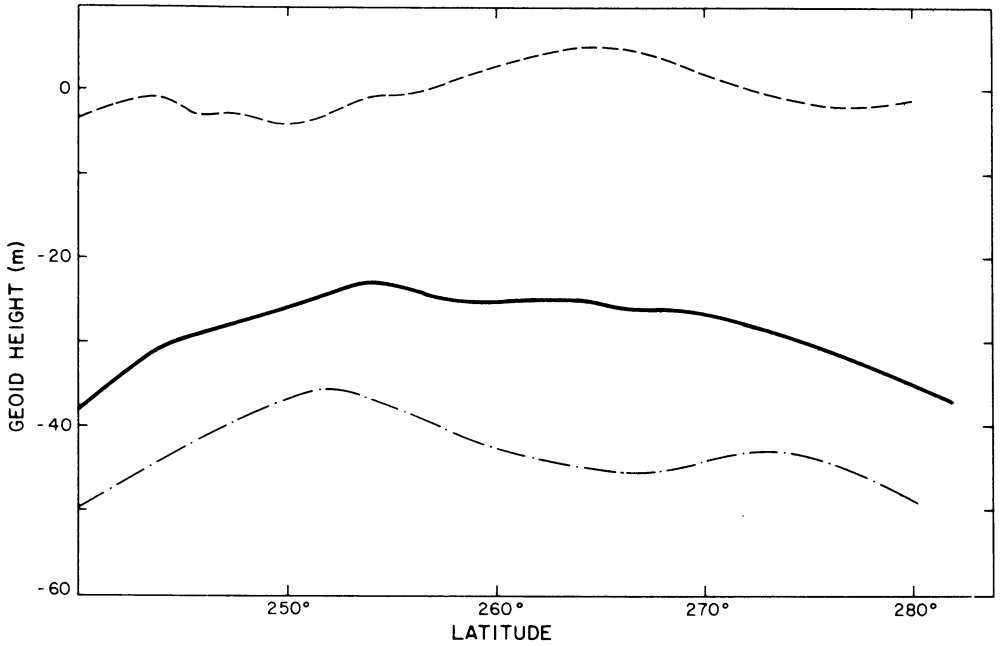

$\phi = 35°$

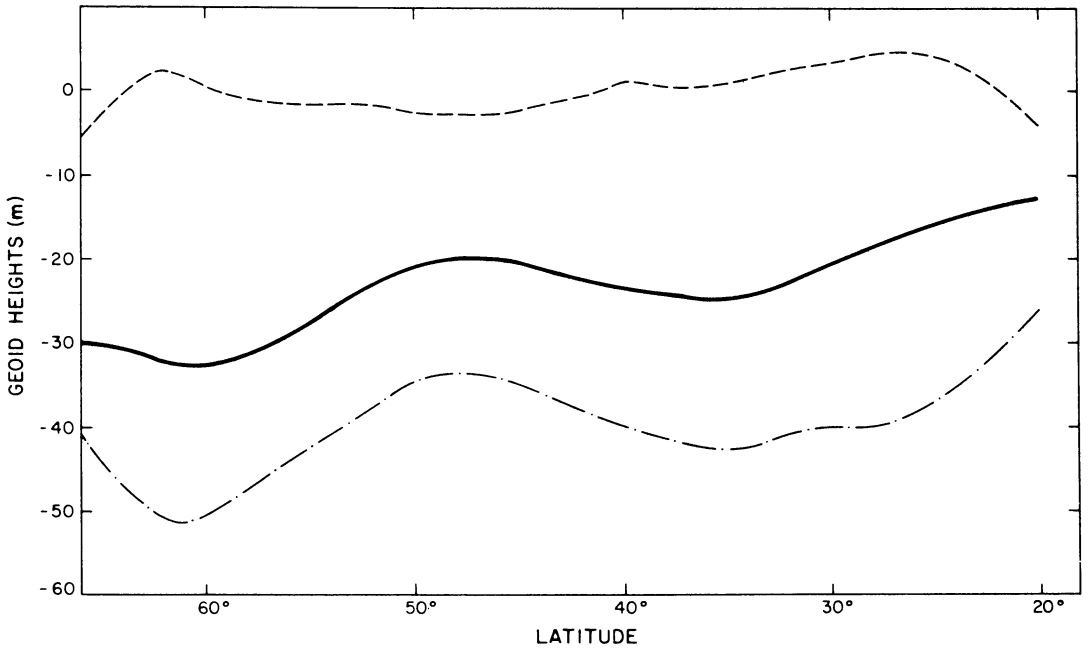

$\lambda = 260°$

North American Datum

Fig. 12. Comparisons between geoid profiles obtained from the combination solution (solid lines) with profiles obtained from astrogeodetic measurements transformed into the global reference system (dashed lines). The difference between the two profiles, after the systematic part has been subtracted, is indicated by the dotted line.

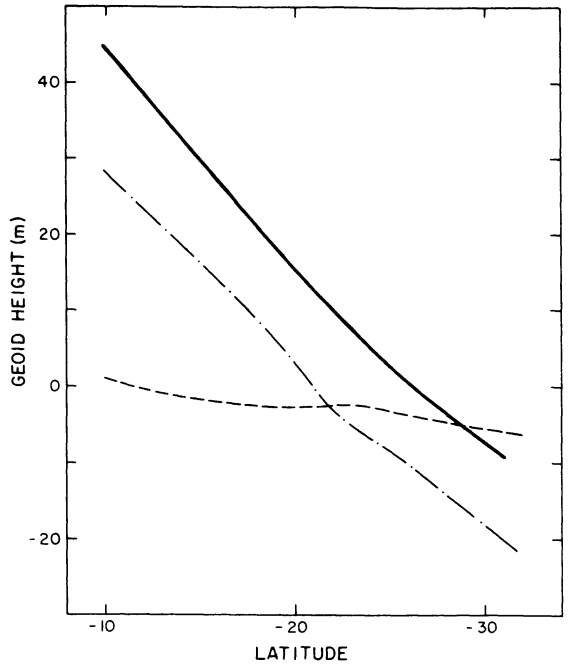

$\lambda = 136.^{\circ}25$

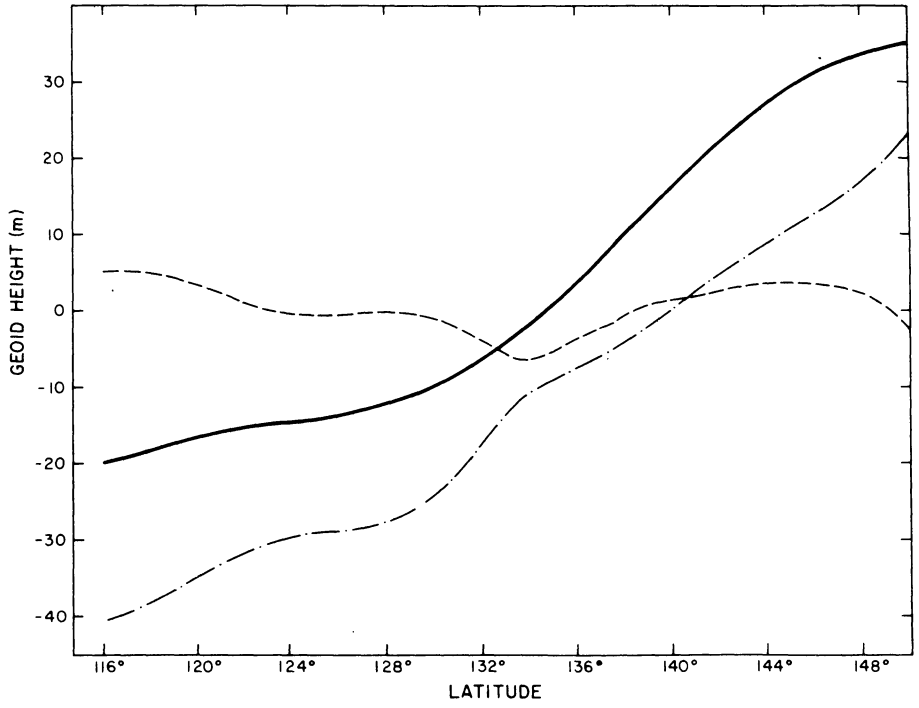

$\phi = -28.^{\circ}75$

Australian Geodetic Datum

Fig. 12 (Cont.)

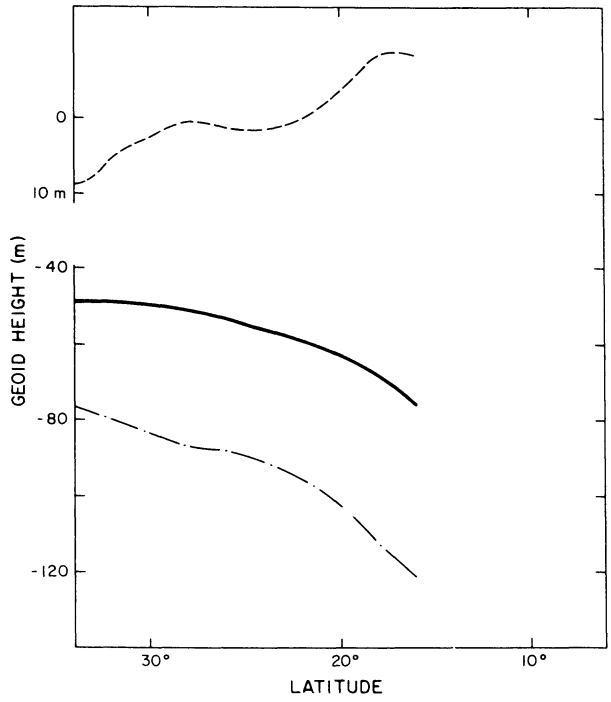

λ = 75°

Indian Datum

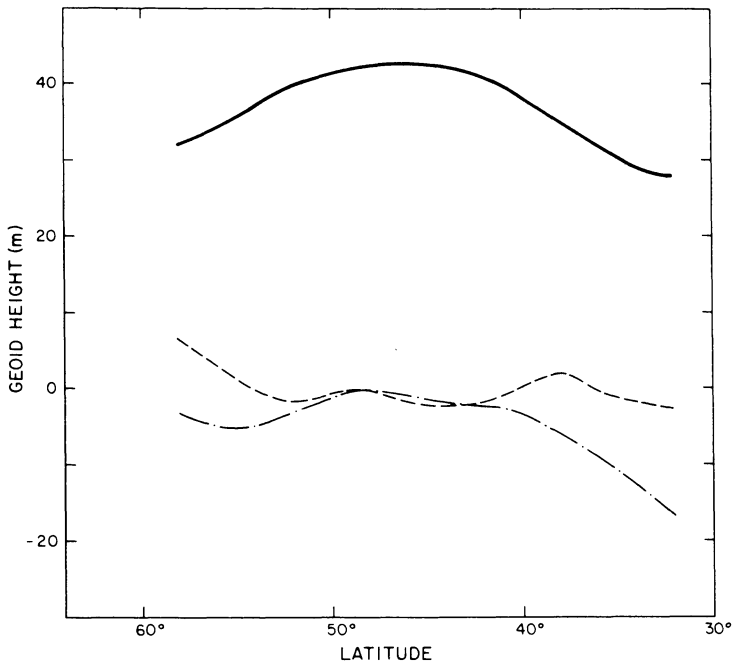

λ = 16°

European Datum

Fig. 12 (Cont.)

TABLE 22. Summary of the comparisons between the geoid profiles obtained from the combination solution and the astrogeoids referred to the geocentric system. $\overline{\Delta h}$ is the systematic height difference between the profiles, $\sigma^2_{\delta h}$ the variance of the difference between the two profiles, σ^2_a the variance of the astrogeoid heights, and σ^2_S the contribution of the combination solution to $\sigma^2_{\delta h}$.

Datum	Profile	$\overline{\Delta h}$	$\sigma^2_{\delta h}$	σ^2_a	$\sigma^2_S = \sigma^2_{\delta h} - \sigma^2_a$
NAD	$\phi = 35°$	-15	8	1.5	6.5
NAD	$\lambda = 260°$	-16	6	1.5	4.5
AGD	$\phi = -28.°75$	-12	10	1.5	8.5
AGD	$\lambda = 136.°25$	-12	12	1.5	10.5
IND	$\lambda = 75°$	-36	30	1.5	28.5
EUR	$\lambda = 16°$	-42	6	1.5	4.5
					$(\sigma^2_S)_{AV} = 10.5\ m^2$

The negative value for $\overline{\Delta h}$ for all the datums considered indicates that the adopted semimajor axis of the reference ellipsoid is too large, by about 15 m as noted, for example, by Veis [1968]. Figure 12 also suggests a possible tilt in the South Asian datum.

Comparison with Terrestrial Triangulation

For stations in North America and Europe where there are extensive surface triangulation nets, it is possible to compare the coordinates of the tracking stations as determined from the combination solution and from terrestrial measurements. But before a comparison can be made, the latter coordinates have to be transferred to a coordinate system coincident with the global geocentric system. These transformations are discussed in Lambeck [1970]. For the present solution, the distances between stations are used as the basis of the comparison. These distances are derived from the surface data scaled by the factors determined from the datum adjustments.

Table 23 summarizes the results. The accuracy estimate is computed from the accuracy estimates of the coordinates for the combination solution and from accuracy estimates of the terrestrial data. The latter have been assumed to be reliable to 1 in 200,000.

TABLE 23. Results of differences Δr and accuracy estimates $\sigma_{\Delta r}$ between interstation distances computed from the combination solution and from surface triangulation after removal of any systematic scale error in the datum.

Line	$\Delta r \pm \sigma_{\Delta r}$	Line	$\Delta r \pm \sigma_{\Delta r}$	Line	$\Delta r \pm \sigma_{\Delta r}$
		Comparisons for European Datum			
8015-9004	8.0 ± 9.0	9004-9080	-2.9 ± 11.8	9066-9080	-5.6 ± 9.4
8015-9065	-11.2 ± 9.6	9004-9091	3.7 ± 13.9	9066-9091	-9.1 ± 9.9
8015-9066	-6.3 ± 3.5	9004-9115	31.8 ± 18.5	9066-9115	27.8 ± 14.2
8015-9077	-4.7 ± 10.4	9065-9066	-4.3 ± 9.5	9077-9080	± 13.4
8015-9080	0.1 ± 9.4	9065-9077	-1.0 ± 13.9	9077-9091	± 9.8
8015-9091	-7.1 ± 9.3	9065-9080	-5.8 ± 10.9	9077-9115	± 15.3
8015-9115	22.6 ± 14.8	9065-9091	-12.6 ± 13.8	9080-9091	-15.8 ± 14.9
9004-9065	14.8 ± 12.9	9065-9115	36.4 ± 14.7	9080-9115	32.1 ± 14.5
9004-9066	2.3 ± 9.7	9066-9077	-1.2 ± 10.3	9091-9115	2.1 ± 17.5
		Comparisons for North American Datum			
1021-1042	-0.7 ± 7.5	1042-7036	3.4 ± 11.0	7045-7075	6.1 ± 13.1
1021-7036	3.5 ± 12.1	1042-9050	15.6 ± 14.2	7045-9050	7.1 ± 17.2
1021-7075	-7.0 ± 9.7	1042-9114	1.5 ± 17.3	7075-9114	-13.7 ± 16.5
1021-9001	-5.6 ± 12.4	7036-7075	17.3 ± 13.8	9001-9010	6.9 ± 11.7
1034-7037	3.0 ± 8.9	7036-9010	4.8 ± 10.3	9001-9050	11.8 ± 17.5
1034-7045	-1.5 ± 9.9	7037-7045	1.8 ± 9.5	9010-9113	3.1 ± 15.1
1034-9010	-1.4 ± 13.0	7037-9001	1.6 ± 8.9	9050-9114	-15.2 ± 20.3
1034-9113	4.9 ± 12.1	7037-9113	1.6 ± 12.1	9113-9114	14.8 ± 15.7

The first part of Table 23 refers to coordinates in the European Datum. All available stations, with the exception of Riga 9074, have been used in this comparison. The second part refers to stations in the NAD. All available

stations were used. For most of the comparisons, $\sigma_r > \Delta r$, indicating that the accuracy estimates given for the coordinates of the combination solution (Table 13) are reliable. For station 9115 the agreement is not so good but always within the 3σ level.

Comparison with the 1966 Standard Earth Coordinates

Table 24 gives the differences in the coordinates determined in the present solution and in the 1966 solution. For these stations the accuracy of the latter solution was estimated as 15 to 20 m, whereas the present solution is considered to be better than 10 m. With a few exceptions the differences fall within these limits. The exceptions are stations 9002, 9003, and the Z component of stations 9007 and 9011. For the first two stations no comparisons or combinations could be made in 1966, but a combination and a comparison with the JPL data were possible in this solution and the results are in excellent agreement (Table 17). As for the other two stations, the 1966 geometric solution gave a very weak determination for the Z components because of the poor geometry of the station distribution. With the relocation of some stations and with more data available, this Z component is determined much better in the present solution and is in good agreement with the results of the dynamic solution. This can be seen from Figure 10 for the line 9007—9029 where the horizontal axis corresponds approximately to the Z axis. For the remaining stations good comparisons and combinations of the geometric and dynamic solutions were possible in the 1966 solution, and as a result, these coordinates are not significantly different from the new determination. This stresses the importance of having the two independent techniques to determine the station positions. The similarity of the differences in the Z coordinates for stations 9002, 9003, 9007, and 9011, all of which lie in south latitudes, suggests that the 1966 dynamic solution may have had some systematic biases in it because of a poor distribution of observations in the Southern Hemisphere.

TABLE 24. Differences in the coordinates as determined in the new solution and in the 1966 Standard Earth solution. The large discrepancies occurred at stations where no comparisons or combinations of independent solutions were possible in the 1966 solution.

Station	X (m)	Y (m)	Z (m)
9001	+ 1.7	- 0.6	+ 1.0
9002	- 0.7	+26.0	+32.1
9003	-26.0	-13.8	+26.5
9004	- 4.7	+ 3.7	- 7.1
9005	+ 4.3	+13.4	-11.3
9006	- 2.2	+ 3.3	+ 8.6
9007	+ 5.6	- 3.4	+27.8
9008	+11.2	- 9.0	- 4.2
9009	+ 8.6	- 3.6	- 4.1
9010	+ 9.2	- 9.2	- 2.5
9011	+14.2	- 4.0	+30.9
9012	+ 1.8	- 6.8	+ 0.7
9114	+ 1.4	+ 8.4	- 8.0
9115	+ 4.9	+14.6	+ 5.6
9117	+ 3.1	+13.9	+ 4.5

8. CONCLUSIONS

1. A combination of the four methods of estimating parameters used in this analysis gives better results than any subset of these methods.

2. The geocentric station positions of the 12 fundamental Baker-Nunn stations and the laser-optical sites at Haute Provence (8015–7815) and Athens (9091–7816) are determined with an accuracy between 5 and 10 m.

3. To improve upon this accuracy more laser data for the dynamic solution and laser-optical simultaneous data for the geometric solution are required. An improvement in the knowledge of UT1 is also necessary.

4. The geopotential has been determined complete through $\ell = 16$, $m = 16$. Comparisons with surface gravity indicate that up to 10, 10 the satellite solution is about as good as can be expected but that some of the higher terms are poorly determined. The terms between degrees 11 and 16 are determined largely from the surface-gravity data. The M1 8, 8 solution is not improved upon by the new solution truncated at 8, 8.

5. Comparisons with independent data sets indicate that the generalized geoid is reliable to about 3 m.

6. To improve the satellite gravity-field determination for terms beyond $\ell = 11$, more satellites in lower orbits, at distinct inclinations, and tracked with greater precision and uniformity are required.

9. REFERENCES

Aardoom, L., A. Girnius, and G. Veis, Geometric methods, in Geodetic Parameters for a 1966 Smithsonian Institution Standard Earth, vol. 1, edited by C. A. Lundquist and G. Veis, pp. 63-75, Smithsonian Astrophys. Obs. Spec. Rep. No. 200, 1966.

Anderle, R. J., Geocentric positions of sites based on Doppler satellite observations made under the auspices of the Commonwealth of Australia, National Weapons Laboratory Rep. No. 2126, 14 pp., 1967.

Baarda, W., Statistical concepts in geodesy, Publ. Netherlands Geodetic Commission, New Series, vol. 2, No. 4, 1967.

Baarda, W., A testing procedure for use in geodetic networks, Publ. Netherlands Geodetic Commission, New Series, vol. 2, No. 5, 1968.

Bomford, G., Geodesy, 2nd ed., Oxford at the Clarendon Press, London, 1962.

Fischer, I., New pieces in the astrogeodetic geoid map of the world, presented at the XIV General Assembly, IUGG, Lucerne, October 1967.

Fischer, I., M. Slutsky, R. Shirley, and P. Wyatt, Geoid charts of North and Central America, Army Map Service Tech. Rep. 62, 1967.

Fischer, I., and M. Slutsky, A preliminary geoid chart of Australia, Austral. Surv., 21, 237-331, 1969.

Gaposchkin, E. M., Tesseral harmonic coefficients and station coordinates from the dynamic method, in Geodetic Parameters for a 1966 Smithsonian Institution Standard Earth, vol. 2, edited by C. A. Lundquist and G. Veis, pp. 105-258, Smithsonian Astrophys. Obs. Spec. Rep. No. 200, 1966.

Gaposchkin, E. M., A dynamical solution for the tesseral harmonics of the geopotential and station coordinates using Baker-Nunn data, in Space Research VII, edited by R. L. Smith-Rose, S. A. Bowhill, and J. W. King, pp. 683-693, North-Holland Publ. Co., Amsterdam, 1967.

Gaposchkin, E. M., Satellite orbit analysis at SAO, in Space Research VIII, edited by A. P. Mitra, L. G. Jacchia, and W. S. Newman, pp. 76-80, North-Holland Publ. Co., Amsterdam, 1968.

Gaposchkin, E. M., Improved values for the tesseral harmonics of the geopotential and station coordinates, presented at XII Meeting of COSPAR, Prague, May 1969.

Gaposchkin, E. M., and K. Lambeck, New geodetic parameters for a standard earth, presented at AGU Meeting, San Francisco, December 1969.

Hagihara, Y., The stability of the solar system, in Planets and Satellites, The Solar System III, edited by G. P. Kuiper and B. M. Middlehurst, University of Chicago Press, Chicago, 1961.

Heiskanen, W. A., and H. Moritz, Physical Geodesy, W. H. Freeman and Co., San Francisco, 1967.

Kaula, W. M., Tests and combination of satellite determinations of the gravity fields with gravimetry, Journ. Geophys. Res., 71, 5303-5314, 1966a.

Kaula, W. M., Theory of Satellite Geodesy, Blaisdell Publ. Co., Waltham, Massachusetts, 1966b.

Kaula, W. M., Global harmonic and statistical analysis of gravimetry, in Gravity Anomalies: Unsurveyed Areas, edited by H. Orlin, pp. 58-67, American Geophysical Union, Washington, D. C., 1966c.

Kaula, W. M., Orbital perturbations from terrestrial gravity data, Final Report, Contract AF(601)-4171, 1966d.

Köhnlein, W. J., Corrections to station coordinates and to nonzonal harmonics from Baker-Nunn observations, in Space Research VII, edited by R. L. Smith-Rose, S. A. Bowhill, and J. W. King, pp. 694-701, North-Holland Publ. Co., Amsterdam, 1967a.

Köhnlein, W. J., The earth's gravitational field as derived from a combination of satellite data with gravity anomalies, Smithsonian Astrophys. Obs. Spec. Rep. No. 264, 57-72, 1967b.

Kozai, Y., The earth gravitational potential derived from satellite motion, Space Sci. Rev., 5, 818-879, 1966.

Kozai, Y., Revised values for coefficients of zonal spherical harmonics in the geopotential, Smithsonian Astrophys. Obs. Spec. Rep. No. 295, 17 pp., 1969.

Lambeck, K., Optimum station-satellite configurations for simultaneous observations to satellites, Smithsonian Astrophys. Obs. Spec. Rep. No. 231, 47 pp., 1966.

Lambeck, K., A spatial triangulation solution for a global network and the position of the North American Datum within it, presented at the AGU Meeting, Washington, D. C., April 1969a.

Lambeck, K., Comparisons and combinations of geodetic parameters estimated from dynamic and geometric satellite solutions and from Mariner flights, presented at the XII Meeting of COSPAR, Prague, May 1969b.

Lambeck, K., On the reduction and accuracy of Baker-Nunn observations, in Reduction of Satellite Photographic Plates, edited by J. Kovalevsky and G. Veis, COSPAR Transactions No. 7, 1969c.

Lambeck, K., Position determination from simultaneous observations of artificial satellites: An optimization of parameters, Bull. Géod., No. 92, 1969d.

Lambeck, K., The relation of some major geodetic datums to a geocentric reference system, Bull. Géod. (in press), 1970.

Lehr, C. G., Geodetic and geophysical applications of laser satellite ranging, IEEE Trans. Geos. Elec., GE-7, 261-267, 1969.

Le Pichon, X., and M. Talwani, Regional gravity anomalies in the Indian Ocean, Deep Sea Res., 16, 263-274, 1969.

Lundquist, C. A., Ed., Geodetic satellite results during 1967, Smithsonian Astrophys. Obs. Spec. Rep. No. 264, 344 pp., 1967.

Lundquist, C. A., and G. Veis, Eds., Geodetic Parameters for a 1966 Smithsonian Institution Standard Earth, Smithsonian Astrophys. Obs. Spec. Rep. No. 200, 3 vols., 1966.

Melbourne, W. G., and D. A. O'Handley, A consistent ephemeris of the major planets in the solar system, Space Programs Summary No. 37-51, vol. III, pp. 4-18, Jet Propulsion Laboratory, Pasadena, California, 1968.

Mottinger, N., Status of D.S.F. location solution for deep space probe missions, Space Programs Summary No. 37-60, vol. II, pp. 77-89, Jet Propulsion Laboratory, Pasadena, California, 1969.

Rapp, R., Analytical and numerical differences between two methods for the combination of gravimetric and satellite data, Boll. Geofis. Teor. Appl., XI, No. 41-42, 108-118, 1969.

Rice, D. A., A geoidal section in the United States, Bull. Géod., 65, 243-251, 1962.

Survey of India, Geodetic Report for 1957, 1957.

Talwani, M., and X. Le Pichon, Gravity field in the Atlantic Ocean, in The Earth's Crust and Upper Mantle, edited by P. J. Hart, American Geophysical Union, Washington, D. C., 1969.

Tienstra, J. M., Theory of the Adjustment of Normally Distributed Observations, N. V. Uitgeverij "Argus," Amsterdam, 1956.

Trask, D. W., and C. J. Vegos, Intercontinental longitude differences of tracking stations as determined from radio tracking data, in Continental Drift, Secular Motion of the Pole, and Rotation of the Earth, edited by W. Markowitz and B. Guinot, D. Reidel Publ. Co., Dordrecht-Holland, 1968.

Uotila, U. A., Investigations on the gravity field and shape of the earth, Publ. Inst. Geod. Photog. Cartog., Ohio State Univ., 10, 92 pp., 1960.

Vegos, C. J., and D. W. Trask, Tracking station locations as determined by radio tracking data, Space Programs Summary No. 37-43, vol. III, Jet Propulsion Laboratory, Pasadena, California, 1967.

Veis, G., Relation with DSIF stations, in Geodetic Parameters for a 1966 Smithsonian Institution Standard Earth, vol. 3, edited by C. A. Lundquist and G. Veis, pp. 115-125, Smithsonian Astrophys. Obs. Spec. Rep. No. 200, 1966.

Veis, G., Geodetic interpretation of the results, in Space Research VII, edited by R. L. Smith-Rose, S. A. Bowhill, and J. W. King, pp. 776-777, North-Holland Publ. Co., Amsterdam, 1967a.

Veis, G., Results from geometric methods, in Space Research VII, edited by R. L. Smith-Rose, S. A. Bowhill, and J. W. King, pp. 778-782, North-Holland Publ. Co., Amsterdam, 1967b.

Veis, G., The determination of the radius of the earth and other geodetic parameters as derived from optical satellite data. Bull. Géod., 89, 253-275, 1968.

Whipple, F. L., On the satellite geodesy program at the Smithsonian Astrophysical Observatory, in Space Research VII, edited by R. L. Smith-Rose, S. A. Bowhill, and J. W. King, pp. 675-683, North-Holland Publ. Co., Amsterdam, 1967.